

# UVM ScholarWorks

## Exploring the Mechanisms of PKG1- $\alpha$ Activation By Synthetic Peptides

Item Type	thesis;article
Authors	Cronin, Connor
Download date	2026-05-13 00:55:56
Link to Item	<a href="https://hdl.handle.net/20.500.14849/3477">https://hdl.handle.net/20.500.14849/3477</a>

EXPLORING THE MECHANISMS OF PKG1- $\alpha$  ACTIVATION BY SYNTHETIC  
PEPTIDES

A Thesis Presented

by

Connor Cronin

to

The Faculty of the Graduate College

of

The University of Vermont

In Partial Fulfillment of the Requirements  
for the Degree of Master of Science  
Specializing in Pharmacology

May, 2022

Defense Date: March 30, 2022  
Thesis Examination Committee:

Wolfgang Dostmann, Ph.D., Advisor  
Margaret Vizzard, Ph.D., Chairperson  
George Wellman, Ph.D.  
Benedek Erdos, Ph.D.  
Cynthia J. Forehand, Ph.D., Dean of the Graduate College

## ABSTRACT

Cyclic GMP-dependent protein kinases (PKG's) are essential signaling macromolecules which play a pivotal role in vascular physiology and smooth muscle tone regulation. As principle downstream effectors of the secondary messenger cyclic 3', 5'-guanosine-monophosphate (cGMP), PKG isoforms are expressed in high levels in all types of smooth muscle cells. The broad range of cellular functions effected by PKG include platelet aggregation, hypertrophy, apoptosis, neuronal plasticity, gene expression, differentiation, vasorelaxation, vascular remodeling, calcium homeostasis, and cardiac function. Recently, a newly characterized helical switch domain within the alpha isoform of PKG (PKG1- $\alpha$ ) has led to the development of S1.1, a novel cGMP-independent peptide activator of PKG1- $\alpha$ . The ability to activate PKG1- $\alpha$  independent of cGMP could have great significance in the development of therapeutics which target vascular smooth muscle. The molecular mechanism behind S1.1 activation of PKG1- $\alpha$  remains unclear. However, a series of S1.1 derivatives have begun to elucidate the synthetic peptide (S-tide) pharmacophore. Until now, the canonical theory of the S-tide pharmacophore involved hydrophobic interactions provided by two phenylalanine residues within the S-tides that are analogous to a portion of the parent enzyme which has been labeled the knob motif. This hypothesis was largely based on the results of previous experiments which showed a complete loss of activity with S1.6, a derivative lacking the phenylalanine residues.

The work displayed in this thesis aims to question the current theory of the synthetic peptide pharmacophore and instead suggest that the loss of activity observed with S1.6 was a consequence of the radioactive kinase assay that was being used to measure activity. By using a slight deviation in methodology, it has been shown that it is possible to drastically alter S-tide activation kinetics. The implications of this are that the apparent S-tide kinetic profile has varied wildly across studies based on which methodology was being employed. The assay component responsible for this shift in activity was isolated through iterative deconstruction of the assay and determined to be magnesium acetate (MgOAc). How MgOAc modulates S-tide activation remains to be discovered, however, these findings are significant and require all past S-tide studies to be examined in a critical light based on these results.

## ACKNOWLEDGEMENT PAGE

I would like to thank all of my committee members, Dr.'s George Wellman, Benedek Erdos, and Margaret Vizzard for each bringing their unique expertise and guidance to this thesis. I would also like to thank the Pharmacology Department, the Accelerated Master's Program (AMP) in Pharmacology, and Tony Morielli the head of the Pharmacology AMP who served as an incredibly kind and helpful advisor throughout my time at the University of Vermont.

I would also like to thank all of the people in the Dostmann lab group, Emily MacDonald, Joseph Charles, Brent Osborne, and especially Wolfgang Dostmann. Wolfgang has taught me an incredible amount about not only pharmacology and science but life in general. He has been instrumental in shaping my future path to California and given me more opportunity than I ever could have dreamed of. He has taught me humility in the face of innumerable defeats in the most complicated, obscure board games known to man. For that I am extremely grateful, I will always treasure the times we had playing board games and talking about life.

## TABLE OF CONTENTS

ACKNOWLEDGEMENT PAGE.....	ii
LIST OF TABLES.....	v
LIST OF FIGURES.....	vi
1.0 INTRODUCTION.....	1
1.1 PKG's Role in the Nitric Oxide Signaling Pathway.....	1
1.2 PKG's Role in Regulating Smooth Muscle Tone.....	3
1.3 Genetic Overview.....	6
1.4 Architecture.....	8
1.5 Switch Domain.....	9
1.6 Synthetic Peptide Activators of PKG1- $\alpha$ .....	14
1.7 S-tide Pharmacophore.....	16
1.8 Aims of the Present Thesis.....	17
2.0 MATERIALS AND METHODS.....	19
2.1 Expression of PKG.....	19
2.2 Synthetic Peptide Synthesis.....	19
2.3 Kinetic Analysis of PKG1- $\alpha$ .....	20
2.4 Normal Assay.....	21
2.5 ATP Preincubation Assay.....	23
2.6 Dilution Assay.....	24
2.7 LSA-50 Papers.....	25
2.8 Data Analysis.....	26
3.0 Results.....	27
3.1 PKG1- $\alpha$ Activation via cGMP.....	27
3.2 Normal Assay Activation Kinetics.....	28
3.7 LSA-50 filter papers as an alternative to phosphocellulose.....	46
4.0 Discussion.....	49
4.1 Assay Conditions Drastically Affect PKG-1 $\alpha$ activation.....	51
4.2 Comparison of Preincubation Methods.....	52
4.3 Kinase Assay Deconstruction.....	53

4.4	Deconstruction of the MES Buffer.....	54
4.5	Revision of S-tide Pharmacophore.....	57
4.6	Small Molecule Derivatives.....	58
5.0	REFERENCES .....	59

## LIST OF TABLES

Table 3.2	Synthetic peptide names and sequences .....	29
Table 3.2.1.	Activation kinetics of S1.5 under the normal preincubation scheme.....	31
Table 3.2.2.	Activation kinetics of S1.6 under the normal preincubation scheme.....	33
Table 3.2.3.	Activation kinetics of Wolf4 under the normal preincubation scheme...	35
Table 3.3.1.	Activation kinetics of S1.6 comparing the normal preincubation and ATP preincubation schemes .....	38
Table 3.3.2.	Activation kinetics of Wolf4 comparing the normal preincubation and ATP preincubation schemes .....	40
Table 3.4.	Activation kinetics of S1.5 comparing the dilution preincubation scheme and the normal preincubation.....	42

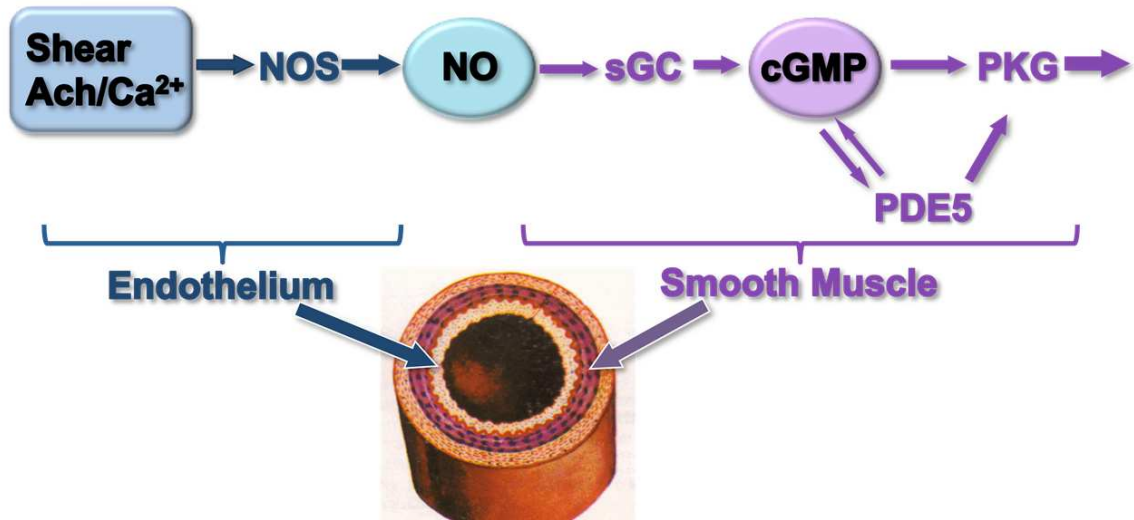
## LIST OF FIGURES

Figure 1.1	Nitric Oxide Signaling Pathway .....	2
Figure 1.2	Signaling Mechanisms of Smooth Muscle Contraction.....	5
Figure 1.3	Alternative Splicing of PRKG1 .....	7
Figure 1.4	General architecture and domain organization of PKG-1 $\alpha$ .....	9
Figure 1.5.1	Crystallized Regulatory Domain of PKG1- $\alpha$ .....	10
Figure 1.5.2.	Structure of the Regulatory Fragment Dimerization Interface.....	12
Figure 2.4	Normal Assay Schematic.....	22
Figure 3.1	cGMP Activation of PKG.....	28
Figure 3.2.1	S1.5-induced activation of PKG1- $\alpha$ .....	30
Figure 3.2.2	S1.6-induced activation of PKG1- $\alpha$ .....	33
Figure 3.2.3	Wolf4-induced activation of PKG1- $\alpha$ .....	35
Figure 3.3.1	A comparison of S1.6 activation curves under Normal and ATP activation	37
Figure 3.3.2	A comparison of Wolf4 activation curves under Normal and ATP activation.....	39
Figure 3.4	S1.5-induced activation of PKG1- $\alpha$ under dilution conditions.....	42
Table 3.5	Status of S1.6-induced PKG activation under varying preincubation conditions.....	44
Figure 3.6	Component Effects of MES Buffer .....	46
Figure 3.7	Comparison of LSA-50 and P81 activation .....	48
Figure 4.4	Helix Wheel Depiction of S1.6 .....	56

## **1.0 INTRODUCTION**

### **1.1 PKG's Role in the Nitric Oxide Signaling Pathway**

As part of the nitric oxide signaling pathway, cyclic guanosine monophosphate (cGMP) dependent protein kinase (PKG) plays a pivotal role in vascular physiology. The nitric oxide signaling pathway starts with the synthesis of nitric oxide, which is generated by multiple different nitric oxide synthase isoforms within the endothelial layer of blood vessels (**Figure 1.1**). The synthesized nitric oxide then activates soluble guanylyl cyclase producing a varying amount of cytosolic cGMP depending on the synthase isoform involved (Sellak et al. 2012). Alternatively, cGMP can be produced via a separate pathway by membrane bound particulate guanylyl cyclase, which is activated by natriuretic peptides instead of nitric oxide. cGMP has several downstream effectors, allowing it to act as a versatile secondary messenger. These downstream effectors can include cGMP-modulated ion channels and phosphodiesterases. However, the primary intracellular receptor of cGMP is the serine-threonine kinase PKG (Light, Stanton, and Corbin 1990, Sellak et al. 2012). The relevance of PKG in the vasculature has been demonstrated via PKG-1 knockout mice which exhibit systemic and pulmonary hypertension, reduced cGMP-dependent vasorelaxation, and severely impacted cardiac, vascular, intestinal, and kidney functions (Zhao et al. 2012, Sellak et al. 2012). The myriad of effects induced by PKG-1 knockout can be attributed to the wide variety of substrates that it targets and numerous protein interactions with its N-terminus. As a result of this, PKG is involved with a wide variety of cellular functions including platelet aggregation, hypertrophy, apoptosis, neuronal plasticity, gene expression, differentiation, vasorelaxation, vascular remodeling, calcium homeostasis, and cardiac function (Francis et al. 2010).



**Figure 1.1. Nitric Oxide Signaling Pathway**

Nitric oxide is synthesized within the endothelium upon activation of NOS. The small-molecule nature of nitric oxide allows it to diffuse through the endothelial layer of blood vessels into vascular smooth muscle tissue and activate soluble guanylyl cyclase, catalyzing the production of cGMP. Cyclic GMP activates both PKG, which goes on to phosphorylate many downstream targets, and PDE5 which serves as a negative feedback loop by degrading cGMP. NOS: Nitric oxide synthase. NO: Nitric oxide. sGC: Soluble guanylyl cyclase. PDE5: Phosphodiesterase type 5. Image adapted with permission from W. Dostmann.

## **1.2 PKG's Role in Regulating Smooth Muscle Tone**

Smooth muscle contractility is heavily correlated with the levels of intracellular calcium present. Increases in intracellular calcium levels within smooth muscle results in the activation of Calcium/calmodulin-dependent myosin light chain kinase and subsequent phosphorylation of the myosin regulatory light chains. This phosphorylation leads to increased myosin ATPase activity and cross-bridge cycling which ultimately stimulates muscle contraction.(Horowitz et al. 1996) The method in which intracellular calcium levels are attenuated to induce muscle contraction is dependent on either influx of extracellular calcium via ion channels and transporters or via a release of calcium from intracellular stores. The latter of which can be mediated by either IP3 regulated channels or via a calcium induced calcium release from ryanodine receptor-regulated channels (Horowitz et al. 1996).

Decreases in intracellular calcium levels results in vasorelaxation. Intracellular calcium levels can be lowered by an extrusion of free calcium by both sodium/calcium exchangers and the sarcolemmal calcium-ATPase. Alternatively, intracellular calcium can be taken up into intracellular stores via the sarcoplasmic reticulum membrane Calcium-ATPase pump. To a lesser degree, specific calcium binding molecules present in both the sarcoplasmic reticulum and the myoplasm can bind calcium and act as a sequestration buffer (Horowitz et al. 1996).

PKG interacts with the mechanisms involving smooth muscle tone in multiple ways. The primary method of regulation involves decreasing the overall concentration of intracellular calcium. PKG facilitates this decrease via phosphorylation of regulator of G-protein signaling 2 (RGS2), phospholamban, inositol triphosphate receptor-associated cGMP kinase substrate (IRAG), and large-conductance, voltage, and calcium-sensitive potassium (BK) channels. Phosphorylation of RGS2 decreases G-protein based IP3 synthesis therefore lowering the overall activation of the IP3 receptors and subsequent calcium release (Nalli et al. 2014). Phospholamban binds to the SR Ca-ATPASE pump (SERCA2) and decreases the pump action, therefore providing a rate limiting step in the contraction/relaxation cycle. PKG acts to phosphorylate phospholamban and disrupt the PLB/SERCA2 interaction resulting in increased calcium re-uptake into intracellular stores (Rigatti et al. 2015). PKG phosphorylation of IRAG inhibits the IP3 induced release of calcium from the intracellular storage of the sarcoplasmic reticulum (Salb, Schinner, and Schlossmann 2011). BKca channels are highly expressed in vascular smooth muscle cells and BKca channel activity is correlated with an efflux of potassium (Plüger et al. 2000). This potassium efflux hyperpolarizes the membrane and subsequently reduces VSMC contraction. Upon activation, PKG phosphorylates BKca channels increasing channel activity and therefore contributing to vasorelaxation (Kyle et al. 2013).

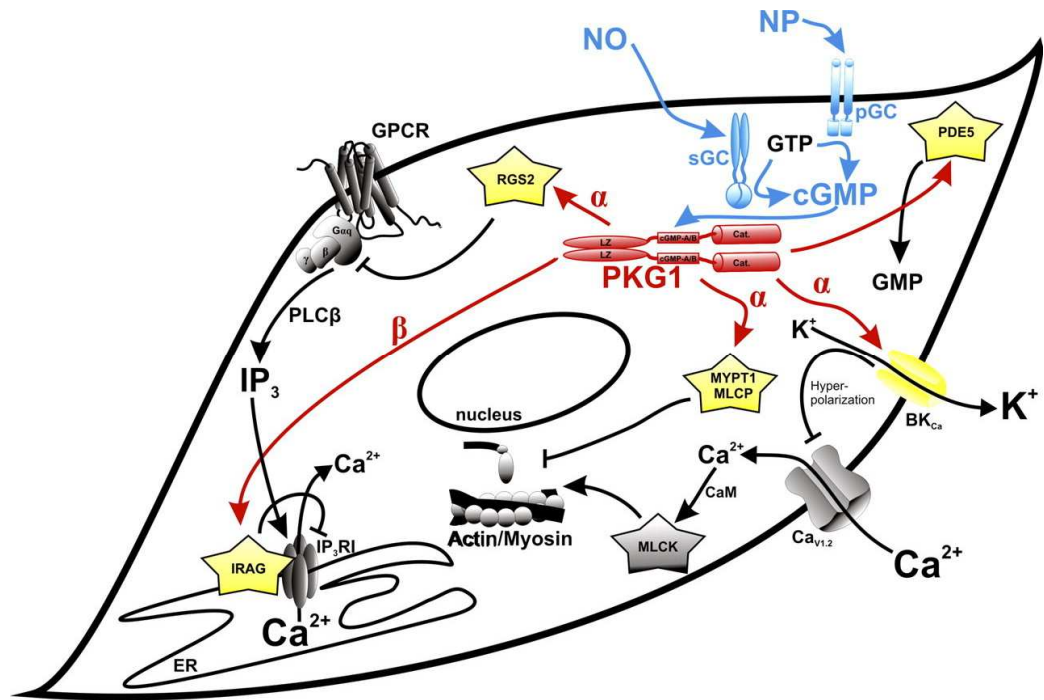


**Figure 1.2. Signaling Mechanisms of Smooth Muscle Contraction**

Cyclic GMP is synthesized via the nitric oxide (NO) or natriuretic peptide (NP) signaling pathway shown in cyan and then activates cGMP-dependent protein kinase 1 (PKG-1; red). Isoform-specific phosphorylation of PKG-1 substrates (yellow) leads to both a reduction in cytosolic calcium and a desensitization of the smooth muscle contraction apparatus, resulting in relaxation of the vascular smooth muscle. PDE5: phosphodiesterase 5; BK<sub>Ca</sub>: calcium-sensitive potassium channels; MLCK: myosin light chain kinase; RGS2: regulator of G-protein signaling 2; PLCβ: Phospholipase C beta isoform; IP<sub>3</sub>RI: inositol 1,4,5-triphosphate (IP<sub>3</sub>) receptor; CaM: calmodulin; MYPT1: myosin phosphatase targeting subunit 1; sGC: soluble guanylyl cyclase; pGC: particulate guanylyl cyclase; IRAG: inositol trisphosphate receptor-associated cGMP-kinase substrate. Image adapted from Schlossman and Desch 2011.

### 1.3 Genetic Overview

Mammalian cells possess two PKG genes, *prkg1* and *prkg2*, which encode for the PKG-1 and PKG-2 enzymes respectively (Sellak et al. 2012). Southern blot analysis of DNA from human-rodent somatic cell hybrids have shown that *prkg1* is assigned to chromosome region 10 and further southern blot analysis of the human genome has shown it to be a single-copy gene (Tamura et al. 1996, Sellak et al. 2012). The *prkg1* gene consists of 19 exons, the first two of which have been identified as being unique to two isoforms  $\alpha$  and  $\beta$ . The amino acid sequence from amino acid 90 to the C-terminus of PKG-1 $\alpha$  is identical to the amino acid sequence from amino acid 105 to the C-terminus of PKG-1 $\beta$ . The N-terminal region shows homology between amino acids of the two isozymes of 36%. This suggests that the PKG-1 $\alpha$  and PKG-1 $\beta$  isoforms are generated by alternative splicing of the single gene on chromosome 10 (Tamura et al. 1996). Importantly, the apparent binding affinity of PKG-1 for cGMP differs by a factor of tenfold amongst the isozymes, with PKG-1 $\alpha$  ( $10^{-4}$  mol/L) having one tenth that of PKG-1 $\beta$  ( $1.3 \times 10^{-3}$  mol/L) (Butt et al. 1993). This must be a result of the difference in the N-terminal regions of the isozymes, which contain the dimerization domain and autophosphorylation sites.

Both isoforms of PKG-1 are expressed in high levels in all types of smooth muscle cells such as the uterus, intestine, trachea, as well as vascular smooth muscle. PKG-1 $\beta$  is further highly expressed in platelets and at lower levels in endothelial cells whereas PKG-1 $\alpha$  is expressed at lower levels in cardiomyocytes (Das et al. 2015, Sellak et al. 2012).

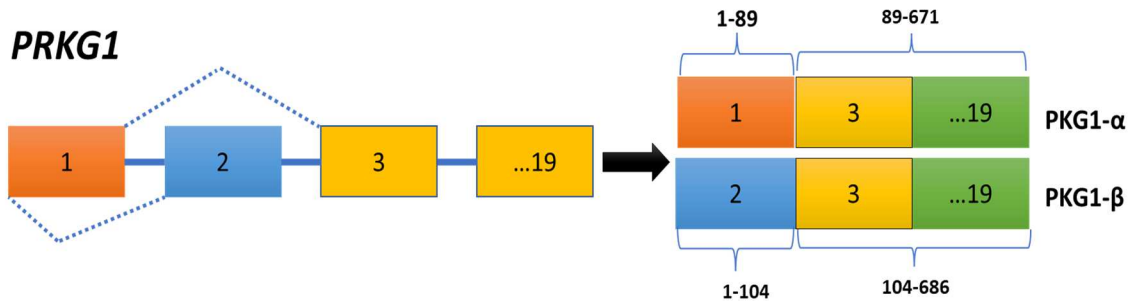


**Figure 1.3. Alternative Splicing of PRKG1**

The *prkg1* gene is a single-copy gene located on chromosome 10 and encodes for cGMP-dependent protein kinase type 1 (PKG1). Two isoforms, PKG1- $\alpha$  and PKG1- $\beta$ , exist as splice variants of the *prkg1* gene. The first two exons of *prkg1* correspond to the two splice variants while the remaining 17 exons are shared between the two isoforms. Amino acids 89-671 in PKG1- $\alpha$  are identical to residues 104-686 in PKG1- $\beta$ . Numbered boxes represent exons, lines between the boxes represent introns, and the dotted lines illustrate the alternative splicing of *prkg1*.

## 1.4 Architecture

PKG exists as a parallel homodimer with a similar domain configuration across all isoforms (PKG-1 $\alpha$ , PKG-1 $\beta$ , PKG-II) (Osborne et al. 2011). Each protomer consists of a dimerization domain, an autoinhibitory domain, a regulatory domain, and a catalytic domain (**Figure 1.4**). The N-termini contains the dimerization domain, a left-handed coiled-coil leucine zipper motif which tethers PKG homodimers together (Schnell et al. 2005). Following the dimerization domain is the autoinhibitory domain, which possesses a pseudo-substrate sequence that acts to autoinhibit the catalytic domain on the C-terminus (Wolfe, Francis, and Corbin 1989). Following the autoinhibitory domain is the regulatory domain which is composed of three components: two tandem cGMP binding sites (A and B) which exhibit positive cooperativity, and a recently discovered helical switch domain thought to be responsible for interchain protomer communication (Osborne et al. 2011). As PKG exists as a parallel homodimer, this makes for four cGMP binding sites in total. One explanation for the necessity of multiple binding sites is posed by the cytotoxic effects of cGMP. It has been shown that high intracellular concentrations of cGMP will induce apoptosis (Lee et al. 2019). The positive cooperativity of the two tandem cGMP binding sites increases the sensitivity of PKG for cGMP and therefore reduces the total intracellular cGMP concentration needed for PKG activation (Osborne et al. 2011). Lastly, the C-terminus contains an ATP binding region followed by a substrate binding region, together forming the catalytic domain of the enzyme. The catalytic domain is autoinhibited via the N-terminal pseudo substrate until the binding of cGMP to both binding sites induces a large conformational change, elongating the molecule and releasing the catalytic domain (Nausch 2008).

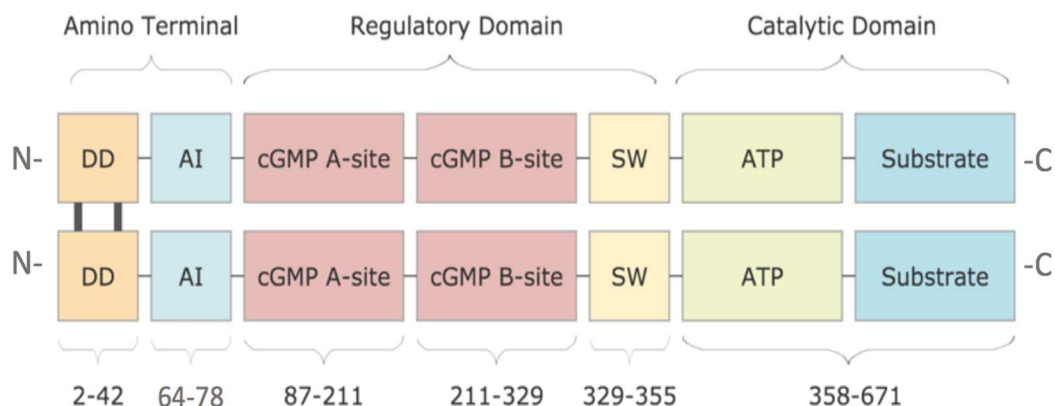


**Figure 1.4. General architecture and domain organization of PKG-1 $\alpha$**

DD: docking and dimerization domain. AI: autoinhibitory domain. cGMP A-site/cGMP B-site: Tandem cGMP binding sites within the regulatory domain. SW: switch helix domain. The black bars within the N-terminus denote the parallel leucine zippers facilitating the parallel homodimerization.

### 1.5 Switch Domain

The switch domain (SW) of PKG1- $\alpha$  is a recent discovery which arose from the crystallization of the regulatory fragment of PKG1- $\alpha$ . Historically, all attempts to crystallize full-length PKG from mammalian cell cultures have been unsuccessful. This is a consequence of mixed phosphorylation sites within the N-terminus leading to conformational heterogeneity, in addition to a proteolytically exposed hinge region at ARG77. Therefore, it was hypothesized that exclusion of both the C-terminal catalytic domain and the N-terminal dimerization domain would give rise to a stable monomeric fragment that could be easily expressed in *Escherichia.coli* and yield diffraction-quality crystals (Osborne et al. 2011). This hypothesis was proven to be correct and resulted in the solving of a 2.5 Å crystal structure of the regulatory domain of PKG1- $\alpha$  (aa78-355; **Figure 1.5.1**), revealing the previously uncharacterized SW helical domain (Osborne et al. 2011).

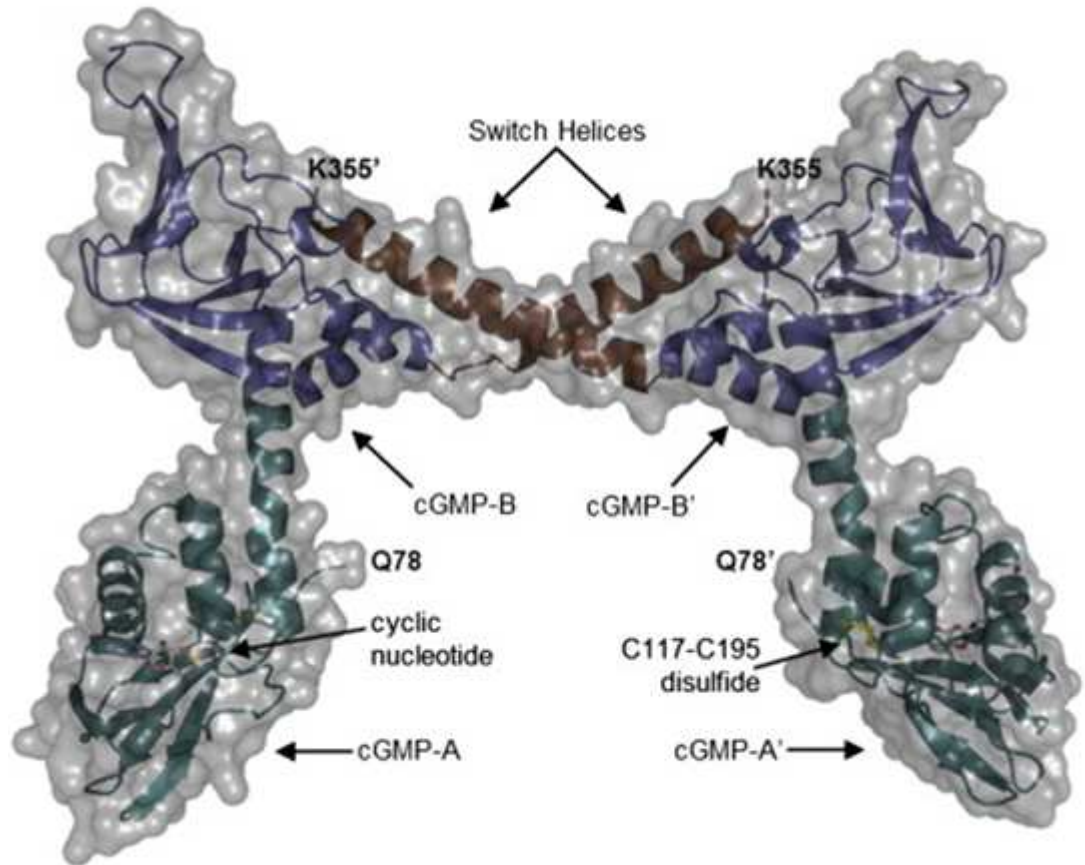


**Figure 1.5.1. Crystallized Regulatory Domain of PKG1-  $\alpha$**

The crystallized regulatory fragment of PKG1- $\alpha$  (aa78-355) is displayed in symmetrical dimerized form. Opposing protomers interact via an interface formed between the switch helices and the cGMP-B domain. A disulfide bridge is between C117 of the A helix and C195 of the B helix. The A-domain is cyclic nucleotide-bound by cAMP. Q78 and K355 represent the respective ends of the polypeptide chain. Image adapted with permission from W. Dostmann.

Discovery of the switch helix revealed a site of intermolecular communication that was distinct from the leucine zipper motifs of the N-terminal DD domain. This intermolecular communication is facilitated via a hydrophobic “knob” at the end of the SW (aa350-354) and a hydrophobic “nest” composed of eight noncontiguous residues within the cGMP B-site (**Figure 1.5.2**). The SW extends from the B-site with the PHE350, PHE351, and LEU354 knob sidechains of one protomer interacting with and filling the void of the hydrophobic nest pocket of the opposing protomer. The ASN353 residue of the knob further strengthens this interaction by forming a hydrogen bond with the backbone carbonyl of THR220 within the B-site (Osborne et al. 2011).

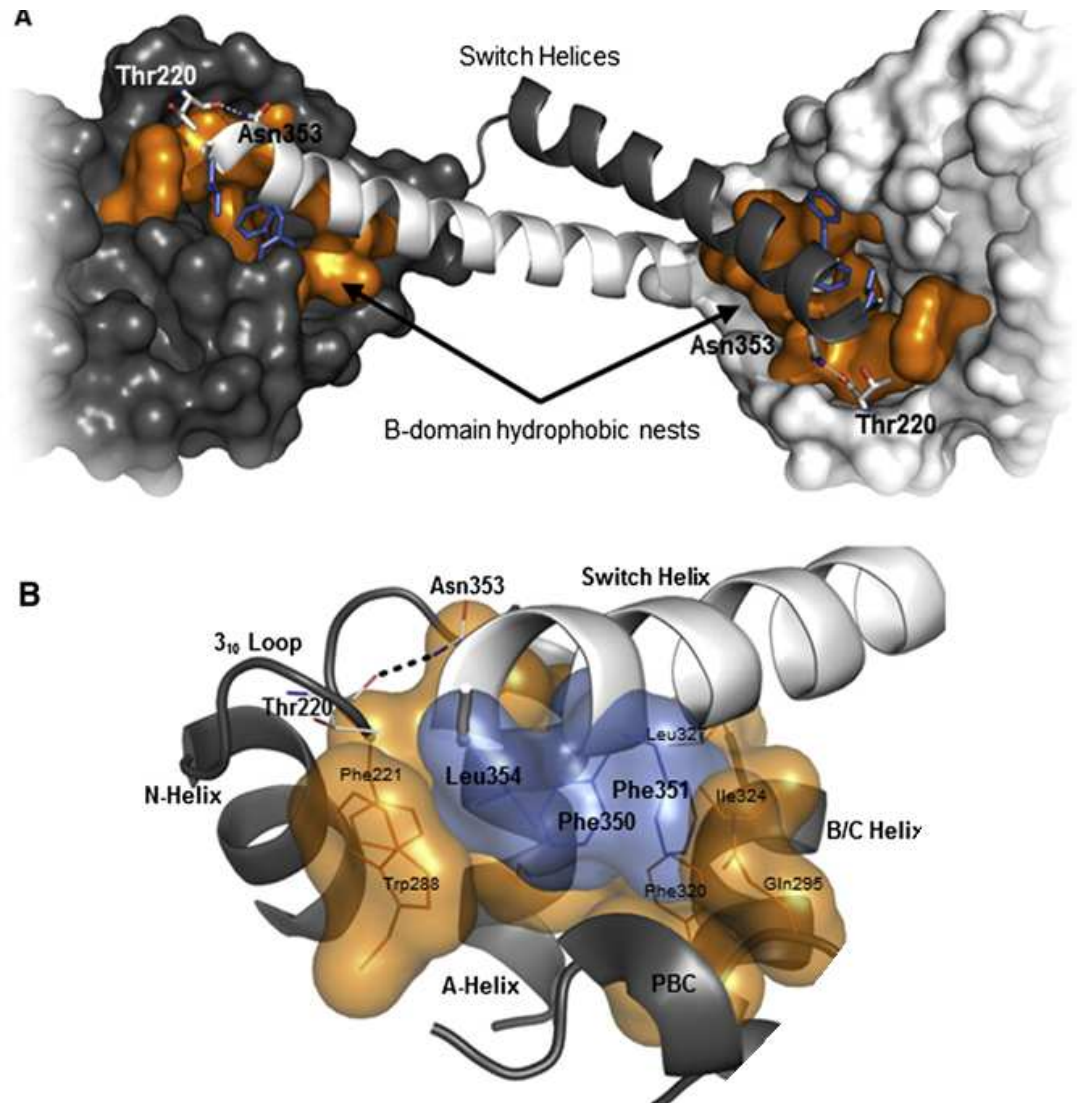


**Figure 1.5.2. Structure of the Regulatory Fragment Dimerization Interface**

(A) Orthogonal view of the switch helices and their interprotomer assemblage with neighboring B-domain hydrophobic nests (orange). The ends of the switch helices consist of hydrophobic knob residues (blue) and a hydrogen bond formed by Asn353 with the backbone carbonyl of Thr220.

(B) Zoomed in view of the knob-nest interaction which facilitates regulatory fragment (PKG<sup>78-355</sup>) dimerization. The hydrophobic knob residues (blue) of the switch helix (white) fill in the hydrophobic pocket created by the B-domain hydrophobic nests (orange). Images adapted with permission from W. Dostmann.

The exact functional relevance of the SW domain remains to be elucidated but one hypothesis suggests that it acts as a tether for the catalytic domain and disruption of this tether allows PKG to be more easily activated. This is evidenced by mutational analysis of HEK293-derived wild-type PKG1- $\alpha$  via alanine scanning mutagenesis of the SW domain. It was shown that mutation of the ASN353 residue, which forms a hydrogen bond between the knob and the THR220 residue from the B-site, results in increased sensitivity of PKG1- $\alpha$  to the endogenous activator cGMP (Osborne et al. 2011). Further mutational analysis shows that a variant of PKG1- $\alpha$  with substitutions of hydrophobic knob residues PHE350, PHE351, and LEU354 in addition to the ASN353 mutation further reduced the activation constant of PKG1- $\alpha$  more than fourfold, from 67 nM to 15.3 nM. Interestingly, this variant had a significantly reduced Hill constant, suggesting a loss of cooperativity. This data suggests that disruption of the SW domain can have significant impacts on PKG1- $\alpha$  activity.

## **1.6 Synthetic Peptide Activators of PKG1- $\alpha$**

The discovery of the novel switch helix domain presented a key target for probing the activation kinetics of PKG1- $\alpha$ . Mutational analysis of the hydrophobic knob residues indicated that disruption of the knob-nest interface greatly reduces the activation constant of PKG1- $\alpha$ . Therefore, it was hypothesized that targeting the knob-nest interaction via synthetic, helical peptides (S-tides) would alter the enzymes kinetics (Moon et al. 2015). The full length of the switch domain (aa329-355) was synthesized as the first synthetic peptide, S1.1. Surface plasmon resonance (SPR) was used to characterize the association of S1.1 with PKG1- $\alpha$ . Remarkably, a clear binding event was observed with projected maximal association within 10 minutes (Moon et al. 2015).

After observing that S1.1 associated with PKG1- $\alpha$ , the effect of this association was probed via a radioactive kinase activation assay. Data from the kinase assay showed that not only did S1.1 associate with PKG1- $\alpha$  but activated it as well. S1.1 activation was cooperative, had an activation constant of 35  $\mu$ M, and reached a maximal velocity of 80% in comparison with cGMP controls (Moon et al. 2015).

A series of peptide derivatives were then synthesized based on the parent S1.1 compound. The first of which (S1.2) was a truncated version of S1.1 with the first three C-terminal residues deleted. Activation potency of the peptide was unaffected ( $K_a=35$   $\mu$ M) yet the maximal velocity was reduced from 80% to 60%. Three more C-terminal residues were deleted (S1.3) resulting in a complete loss of kinase activity. These residues (aa 349-352) comprised most of the knob portion of the switch domain and the loss of activity indicated that they are important for peptide-induced kinase activation. To further probe the importance of these knob residues, a peptide was synthesized (S1.6) containing a double alanine substitution of two phenylalanine knob residues (F350 and F351). It was shown that S1.6 had equivalent activation to that of S1.3, where the knob was deleted instead of mutated.

The N-terminal of S1.1 was then probed via similar three-length amino acid truncations. The first three N-terminal amino acids were removed (S1.4), resulting in increased potency ( $K_a= 12\mu$ M). A further three N-terminal acids were removed (S1.5), resulting in an even more potent derivative ( $K_a=3\mu$ M). Further N-terminal truncations of single amino acids (S1.9 and S1.10) reverted potency back to that of S1.1 and a further truncation (S1.11) abolished activity altogether.

## 1.7 S-tide Pharmacophore

The exact method in which the S-tides activate PKG1- $\alpha$  has yet to be elucidated. The proximity of the nest domain to the cGMP B-site has led to the hypothesis that the S-tide binding site interacts with and is co-dependent with the cGMP B-site. However, this was ruled out via the reduced activation kinetics of an S1.5 analog that had been designed from a molecular modeling approach to interact with the cGMP B-site (Charles 2019). Furthermore, both the S-tide and cGMP activation kinetics were unaffected in a PKG1- $\alpha$  mutant lacking the ability to bind cGMP to the B-site (Moon et al. 2018).

Previously, it has been postulated that S-tide induced activation of PKG1- $\alpha$  was reliant on two contiguous phenylalanine residues (PHE350 and PHE351) that are analogous to a portion of the hydrophobic knob in the native protein. The importance of these phenylalanine's to peptide activation was probed via alanine scanning mutagenesis of the original full-length synthesized switch helix domain (S1.1). Both phenylalanine residues of S1.1 were mutated to alanine, giving rise to the S1.6 peptide. In theory, if the phenylalanine residues are important to the peptide mode of activation, then mutation of them should alter the activation kinetics. Indeed, this was shown to be the case. The S1.6 peptide had a drastically increased activation constant and markedly reduced activation velocity. Future importance of the phenylalanine residues is evidenced by the complete loss of activity displayed in S1.3, the truncated version of S1.1 which is lacking the phenylalanine's altogether. These results were, in large part, the reason behind why it was thought that the phenylalanine residues constituted a portion of the peptide pharmacophore.

## **1.8 Aims of the Present Thesis**

Previous research has explored derivatives of the SW helix S1.1 peptide and isolated certain residues key for peptide activity, yet some discrepancies exist between the contexts of the full-length S1.1 parent peptide and the truncated derivatives. It appeared that substitution of the two phenylalanine residues in the context of the full-length S1.1 peptide would abolish peptide activity, however substitution of the same residues within the context of the truncated S1.5 derivative would have no perceived effects. Therefore, the initial aim of this study was to verify that substitution of the phenylalanine residues results in differing effects on S-tide activation within the contexts of S1.1 and S1.5. This was accomplished by utilizing a radioactive kinase activation assay to quantify the activation kinetics of the S-tide derivatives.

It was very quickly discovered that the hypothesis of the phenylalanine residues having different effects across the full-length and truncated derivatives was incorrect. The data reported in this thesis shows that the full-length S-tide containing the phenylalanine substitutions (S1.6) was not inactive after all and instead possessed activity equivalent to that of S1.5. This was in stark contrast to previously reported values of S1.6 activation that showed no activity (Moon et al. 2015). Therefore, the aim of this project shifted to determining why the S1.6 peptide now displays activity when before it did not.

A deviation in methodology was discovered within the study that reported S1.6 as being inactive. Components of the reaction mix of the radioactive kinase assay had been shifted to the preincubation mix. This deviation caused the S1.6 peptide to appear inactive using one preincubation scheme and active using a different one. As a result, the kinase assay was re-evaluated and the component responsible for the shift in activity was isolated. This was accomplished via a piecewise deconstruction of the assay. The consequences of the assay methodology affecting the perceived peptide activity calls for a complete revision of the S-tide pharmacophore and the results of each past experiment contextualized based on how the assay was performed.

## **2.0 MATERIALS AND METHODS**

### **2.1 Expression of PKG**

The PKG1- $\alpha$  used in these experiments is recombinant and was previously expressed utilizing the Sf9 insect cell Bac to Bac baculovirus expression system (Invitrogen) with a polyhistidine-tag added (Charles 2019). The purification of PKG1- $\alpha$  was accomplished via nickel affinity chromatography. Other methods of purification such as a cGMP-Agarose column would not be suitable for these experiments, as there would be traces of cGMP bound to PKG1- $\alpha$  causing it to be constitutively active.

### **2.2 Synthetic Peptide Synthesis**

Peptides used in this study were synthesized as outlined by Moon et al. 2015 with a Syro multiple peptide synthesizer (MultiSynTech, Witten, Germany) at a scale of 50  $\mu$ mole on Rapp S RAM resin (Rapp Polymere, Tubingen, Germany). Fmoc solid-phase chemistry with 2-(1H-Benzotriazole-1-yl)-1,1,3,3-tetramethylaminium tetrafluoroborate (TBTU) / diisopropylethyl amine activation was employed with tenfold excess. Coupling time was 1 h. Peptides were cleaved and deprotected via a 3 hour treatment with TFA containing 3% triisopropylsilane and 2% water (10 ml/g resin). After precipitation with t-butylmethyl ether, the resulting crude peptides were purified by preparative HPLC (RP-18) with water/acetonitrile gradients containing 0.1% TFA and characterized by MALDI-MS. Final products were lyophilized from water.

### **2.3 Kinetic Analysis of PKG1- $\alpha$**

The kinetic parameters of the purified recombinant PKG 1a upon addition of an activator was tested via two similar radioactive phosphotransferase assays, the Normal assay and the ATP assay. The Normal assay is an adapted form of a radioactive phosphotransferase assay as outlined by Dostmann et al. (2000). The ATP assay is identical to the Normal assay in every way except for the preincubation method, as outlined by Moon et al. (2015). In both assays PKG1- $\alpha$  catalyzes the transfer of the terminal phosphate of a radioactive tagged [ $\gamma$ - $^{32}$ P] ATP to the serine residue of the highly specific substrate TQAKRKKSLAMA-amide (W15) (Dostmann et al. 1999).

There are multiple methods of measuring kinase activity, such as fluorometric assays which correlate enzyme activity with changes in absorption. An example of this is the lactate dehydrogenase (LDH) activity assay which quantifies LDH activity in various biological samples by detecting changes in absorption at 450 nm, correlating directly to LDH reduction of its substrate (Larsen 2005, Sasaki et al. 1992). In comparison to these assays, the radiometric kinase assay has the distinct disadvantage of using radioactive [ $\gamma$ - $^{32}$ P] ATP. However, in the categories of accuracy, speed, and cost the radiometric assay is unrivaled. Therefore, it has been a staple of PKG assays for over 20 years.

## 2.4 Normal Assay

A preincubation mix containing 10  $\mu\text{L}$  of 10x activator stocks and 23.4 ng of PKG1- $\alpha$  suspended in 20  $\mu\text{L}$  of Enzyme Dilution Buffer (EDB) (1mg/mL BSA Cohn's fraction V, 50 mM NaCl, 1mM TCEP, 50mM MES ph 6.9) was preincubated for 30 minutes at 30°C in 1.5 mL Eppendorf tubes. Reactions were initiated via the addition of 70  $\mu\text{L}$  reaction mix containing 20  $\mu\text{L}$  MES mix (250 mM MES, 50mM NaCl, 5mM MgOAc), 10  $\mu\text{L}$  100 mM DTT, 10 $\mu\text{L}$  10mg/mL BSA, 10  $\mu\text{L}$  500  $\mu\text{M}$  W15 substrate, 10  $\mu\text{L}$  ddH<sub>2</sub>O, and 10  $\mu\text{L}$  1mM [ $\gamma$ -<sup>32</sup>P]ATP (200-300 cpm/pmol). Each reaction was run for three minutes at 30°C with a total reaction volume of 100  $\mu\text{L}$ . Reactions were terminated via blotting on 2mm x 1mm phosphocellulose paper filters (Whatman Grade P81 Ion Exchange Cellulose Chromatography Paper, Lab Alley). Filter papers were subsequently washed three times in 0.8% phosphoric acid for five minutes each. A final wash was conducted in acetone for five minutes before being air dried. Filter papers were then suspended in vials containing scintillator fluid (PPO, POPOP, toluene) and radioactivity was measured via liquid scintillation counting (TRI-CARB 4910 110 V Liquid Scintillation Counter, Perkin Elmer). Data from the scintillation readouts was analyzed using Excel (Microsoft) and Prism 8 (GraphPad) and subsequently plotted using Prism 8.

For each set of assays, three controls were used. A preincubation mix containing 10  $\mu\text{L}$  ddH<sub>2</sub>O in lieu of any activator to determine basal enzyme activity, a preincubation mix containing 10  $\mu\text{L}$  of 40  $\mu\text{M}$  cGMP in place of the synthetic peptide as a positive control, and a preincubation mix containing 30  $\mu\text{L}$  ddH<sub>2</sub>O instead of both PKG1- $\alpha$  and an activator as a blank in order to determine basal radiation noise levels.

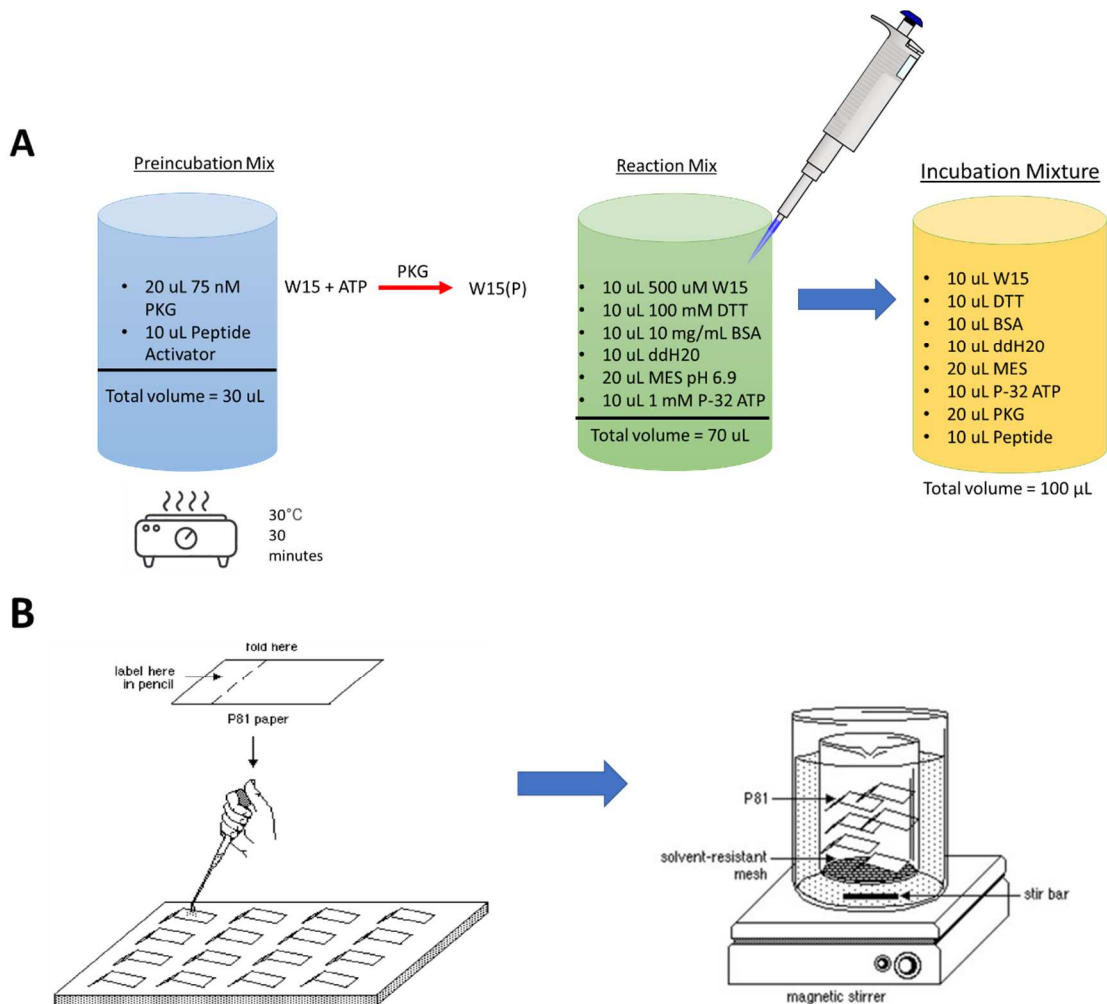


### Figure 2.4 Normal Assay Schematic

(A) The preincubation mix (blue) and reaction mix (green) are depicted containing their respective components. The phosphotransferase reaction is depicted between the two cylinders and is initiated by pipetting the reaction mix into the preincubation mix and incubating at 30°C for 3 minutes.

(B) The reaction is terminated by blotting the incubation mix (yellow) onto P81 phosphocellulose paper. P81 filter papers are then washed three times in 0.8% phosphoric acid for five minutes each. A final wash is conducted in acetone for five minutes.

## 2.5 ATP Preincubation Assay

A preincubation mix containing 10  $\mu\text{L}$  of 10x activator stocks, 23.4 ng of PKG1- $\alpha$  suspended in 20  $\mu\text{L}$  of Enzyme Dilution Buffer (EDB) (1mg/mL BSA Cohn's fraction V, 50 mM NaCl, 1mM TCEP, 50mM MES ph 6.9), 20  $\mu\text{L}$  MES mix (250 mM MES, 50mM NaCl, 5mM MgOAc), 10  $\mu\text{L}$  100 mM DTT, 10 $\mu\text{L}$  10mg/mL BSA, 10  $\mu\text{L}$  500  $\mu\text{M}$  W15 substrate, and 10  $\mu\text{L}$  ddH<sub>2</sub>O ) was preincubated for 30 minutes at 30°C in 1.5 mL Eppendorf tubes for a total preincubation volume of 90  $\mu\text{L}$ . Reactions were initiated via the addition of 10  $\mu\text{L}$  1mM [ $\gamma$ -<sup>32</sup>P]ATP (200-300 cpm/pmol) and then carried out in the same fashion as outlined in the Normal assay. This assay is identical to the Normal assay with the only difference being the constituent components of the reaction mix have been moved to the preincubation mix, except for the [ $\gamma$ -<sup>32</sup>P]ATP.

## 2.6 Dilution Assay

A preincubation mix was created containing 10 $\mu$ L of 10x activator stocks, 23.4 ng of PKG1- $\alpha$  suspended in 20  $\mu$ L of EDB, 16 $\mu$ L of 10mg/mL BSA, and 44  $\mu$ L ddH<sub>2</sub>O for a total volume of 90  $\mu$ L. Preincubation samples were preincubated for 30 minutes at 30°C in 1.5 mL Eppendorf tubes. Reactions were initiated via the addition of 112  $\mu$ L reaction mix containing 32  $\mu$ L MES mix (250 mM MES, 50mM NaCl, 5mM MgOAc), 16  $\mu$ L of 100 mM DTT, 16  $\mu$ L of 500  $\mu$ M W15 substrate, 32  $\mu$ L of ddH<sub>2</sub>O, and 16  $\mu$ L 1mM [ $\gamma$ -<sup>32</sup>P]ATP (200-300 cpm/pmol). Reactions were incubated for 3 minutes at 30°C before being terminated by pipetting 50  $\mu$ L reaction mix onto 2mm x 1mm phosphocellulose paper filters (Whatman Grade P81 Ion Exchange Cellulose Chromatography Paper, Lab Alley). Samples were then washed and analyzed in the same method outlined in **section 2.2**.

## 2.7 LSA-50 Papers

A preincubation mix containing 10  $\mu\text{L}$  of 10x activator stocks and 23.4 ng of PKG1- $\alpha$  suspended in 20  $\mu\text{L}$  of Enzyme Dilution Buffer (EDB) (1mg/mL BSA Cohn's fraction V, 50 mM NaCl, 1mM TCEP, 50mM MES ph 6.9) was preincubated for 30 minutes at 30°C in 1.5 mL Eppendorf tubes. Reactions were initiated via the addition of 70  $\mu\text{L}$  reaction mix containing 20  $\mu\text{L}$  MES mix (250 mM MES, 50mM NaCl, 5mM MgOAc), 10  $\mu\text{L}$  100 mM DTT, 10 $\mu\text{L}$  10mg/mL BSA, 10  $\mu\text{L}$  500  $\mu\text{M}$  W15 substrate, 10  $\mu\text{L}$  ddH<sub>2</sub>O, and 10  $\mu\text{L}$  1mM [ $\gamma$ -<sup>32</sup>P]ATP (200-300 cpm/pmol). Each reaction was run for three minutes at 30°C with a total reaction volume of 100  $\mu\text{L}$ . Reactions were terminated via blotting on 2mm x 1mm LSA-50 papers (Cation exchange paper MN 616 LSA-50 48 mm, CTL Scientific Supply Corp). Filter papers were subsequently washed five times in 0.8% phosphoric acid for five minutes each. A final wash was conducted in acetone for five minutes before being air dried. Filter papers were then suspended in vials containing scintillator fluid (PPO, POPOP, toluene) and radioactivity was measured via liquid scintillation counting (TRI-CARB 4910 110 V Liquid Scintillation Counter, Perkin Elmer). Data from the scintillation readouts was analyzed using Excel (Microsoft) and Prism 8 (GraphPad) and subsequently plotted using Prism 8.

## 2.8 Data Analysis

The exact velocity of PKG1- $\alpha$  can be determined by quantifying the rate at which PKG1- $\alpha$  transfers tagged [ $\gamma$ - $^{32}$ P] ATP to the W15 substrate. The blotting of the reaction mixture onto the P81 phosphocellulose cation exchange paper allows for the adsorption of the positively charged and radioactively tagged substrate onto the paper. The subsequent acetic acid washing steps removes the excess unbound [ $\gamma$ - $^{32}$ P] ATP, leaving the filter paper containing only the radioactively tagged substrate. (Glass et al. 1978)

Therefore, the velocity of the enzyme can be directly correlated to the abundance of the radioactive [ $\gamma$ - $^{32}$ P] ATP present on the filter paper as determined by liquid scintillation counting. In this way, the activation constants for each synthetic peptide can be determined after accounting for the background radiation levels using the blank control. The raw data is obtained from the liquid scintillation counter in counts per minute (CPM). The CPM values are imported into an Excel sheet where the velocity is calculated by multiplying the blotting correction (4.00), which reflects the portion of the incubation mixture that was blotted onto the filter paper, the purity correction (1.02, 98%), and the CPM value. The resulting sum is divided by the reaction time (3 min), protein concentration (23.4 ng), and specific activity resulting in the velocity ( $\mu\text{mol} \times \text{min}^{-1} \times \text{ng}^{-1}$ ). The kinetic constants  $V_{\text{max}}$ ,  $V_{\text{min}}$ , fold activation, and  $K_a$  are calculated by importing the velocities and corresponding activator concentrations into Prism 8 and performing a nonlinear regression on velocity vs log<sub>10</sub> concentration.

### 3.0 Results

#### 3.1 PKG1- $\alpha$ Activation via cGMP

The endogenous activator for PKG1- $\alpha$  is cGMP and therefore it represents a suitable positive control for activity assays. However, there exists some key differences between the activation kinetics of PKG in mammalian cells and the experiments performed within this thesis. It is known that oxidation of PKG increases basal activity, therefore the PKG used in this thesis has been prepared in the presence of TCEP, a strong reducing agent (Gremer 2019). To a lesser degree, the presence of PKA and low levels of cGMP present in vivo further alters the basal activity of PKG. The differences in the environment of PKG in vivo is reflected in a lower  $V_{\min}$  value and consequently a higher fold activation. The in vitro kinetic parameters of cGMP induced PKG activation were probed via a radioactive kinase activation assay (see **section 2.4 Normal Assay**). Results displayed an activation constant of 117 nM and a  $V_{\max}$  value of 4.78  $\mu\text{mol} \times \text{min}^{-1} \times \text{mg}^{-1}$  (**Figure 3.1**). The presence of TCEP allows for a particularly low in vitro  $V_{\min}$  value of around 0.30  $\mu\text{mol} \times \text{min}^{-1} \times \text{mg}^{-1}$ . The fold activation in mammalian cells is around 3, whereas the assays outlined within this thesis display a fold activation that is anywhere between three and fivefold higher. This is important as it offers the ability to filter out background noise and more easily delineate between strong and weak peptide activators.

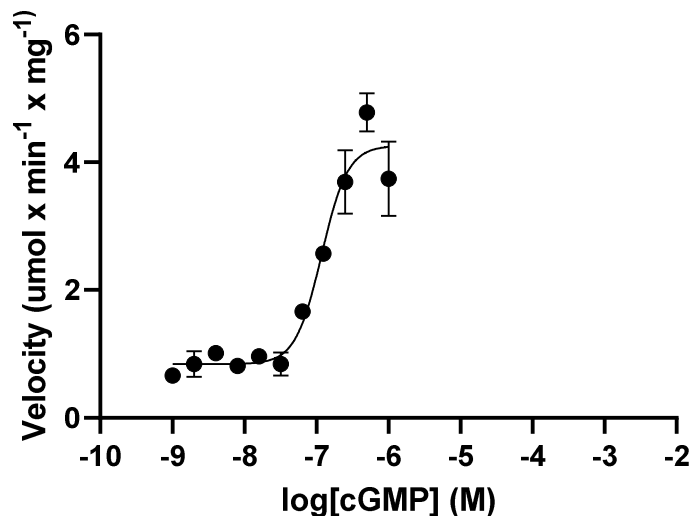


**Figure 3.1 cGMP Activation of PKG**

cGMP induced activation of PKG1- $\alpha$  was measured at varying concentrations under the normal preincubation scheme (shown in black). X-axis concentrations are displayed as a logarithmic function of cGMP concentration.

### 3.2 Normal Assay Activation Kinetics

Radiometric kinase assays were performed using three synthetic peptides (S1.5, S1.6, Wolf4) under the Normal preincubation method. As previously reported, S1.5, the shortened version of the parent switch helix analog S1.1, has consistently shown the most favorable activation kinetics with an activation constant of between 3 and 7  $\mu$ M and a maximal velocity of 80% that of the cGMP control (Moon et al. 2015). In contrast, the S1.1 analog possessing a double phenylalanine substitution (S1.6) has purportedly shown almost nil activity (Moon et al. 2018). The Wolf4 peptide possesses a double phenylalanine substitution akin to that of S1.6, yet in the context of the shorter S1.5 peptide instead of the full length S1.1 switch helix analog (**Table 3.2**). Until now, the activation kinetics of Wolf4 have yet to be probed.

**Table 3.2 Synthetic peptide names and sequences**

Name	Sequence
S1.1	Ac-DVSNKAYEDAEAKAKAYEAEAA <b>FFANL</b> KLSD-NH <sub>2</sub>
S1.5	Ac-YEDAEAKAKAYEAEAA <b>FFANL</b> KLSD-NH <sub>2</sub>
S1.6	Ac-DVSNKAYEDAEAKAKAYEAEAA <b>AAANL</b> KLSD-NH <sub>2</sub>
Wolf4	Ac-YEDAEAKAKAYEAEAA <b>AAANL</b> KLSD-NH <sub>2</sub>

Synthetic peptide names are displayed to the left of their corresponding sequences. Residues in bold are analogous to the knob residues of PKG1- $\alpha$  (aa350-354). Amino acids emboldened in red indicate phenylalanine residues within the analogous knob portion that have been mutated to alanine's.

### 3.2.1 S1.5

The S1.5 peptide is a truncated derivative of the parent S1.1 switch helix peptide, lacking the first six N-terminal amino acids present in S1.1 (**Table 3.1**). Previously, the S1.5 peptide has been thought to be the most potent of the synthetic peptide derivatives and has been a lead candidate for future studies (Charles 2019). Results from the S1.5 assays published within this thesis are inconsistent with reported values, displaying an activation constant of 22.8  $\mu$ M and a Vmax of 5.33  $\mu$ mol (w15-p)/min\*mg (**Figure 3.2.1, Table 3.2.1**). This activation constant is roughly fourfold higher than previously reported values (Moon et al. 2015). It is unclear what caused such a shift in the Ka value.

A decline in activation is observed as the peptide concentration eclipses 62  $\mu\text{M}$ . It is unknown what causes this drop of activity; however, the same effect is seen with cGMP as a result of ATP site occupation at high cGMP levels. It is possible that the S-tides interfere with the substrate binding under high concentrations. The binding mechanism of the peptide displays strong positive cooperativity, as indicated by the Hill slope of 4.18 (Table 3.2.1).

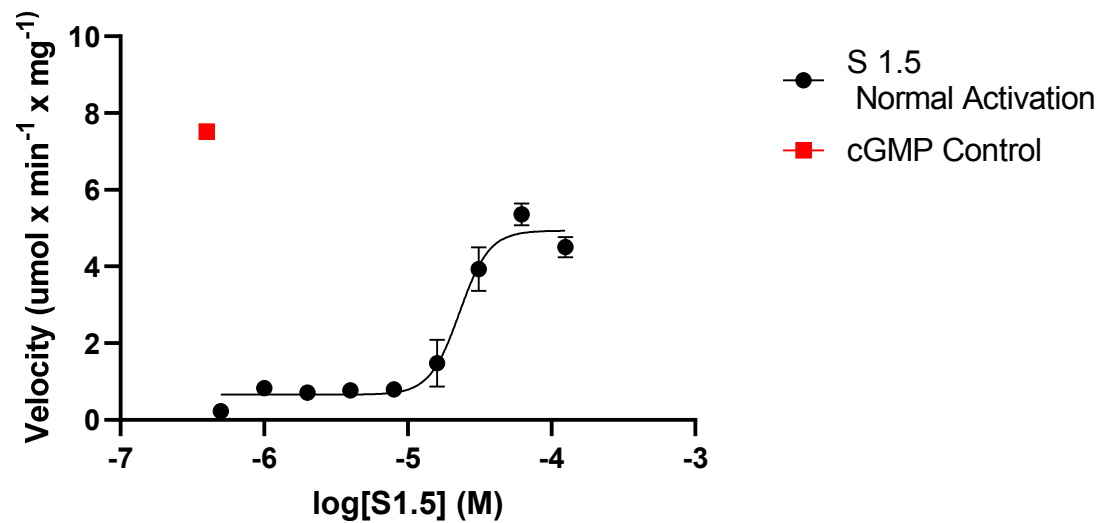


**Figure 3.2.1. S1.5-induced activation of PKG1- $\alpha$**

Activity of PKG1- $\alpha$  was measured at varying concentrations using the S1.5 peptide under the normal preincubation scheme (shown in black). X-axis concentrations are displayed as a logarithmic function of peptide concentration. A positive cGMP control (shown in red) was used at a concentration of 8  $\mu\text{M}$ , corresponding to known values of cGMP  $V_{\text{max}}$ .

**Table 3.2.1. Activation kinetics of S1.5 under the normal preincubation scheme**

Name	V <sub>max</sub>	V <sub>min</sub>	n <sub>H</sub>	K <sub>a</sub> [μM]	N
S1.5 Normal	5.37 ± 0.28	0.23 ± 0.05	4.18	22.9 ± 9.1	6
cGMP	7.52	n/a	n/a	n/a	6

n<sub>H</sub>, Hill coefficient; K<sub>a</sub>, activation constant; N, number of replicates. Velocity units are reported in μmol PKG-1 x min<sup>-1</sup> x mg<sup>-1</sup> substrate.

### 3.2.2 S1.6

The S1.6 peptide was synthesized as a derivative of the parent S1.1 peptide in order to probe the importance of the knob residues of the switch helix. S1.6 is identical to S1.1, other than a double alanine substitution of two phenylalanine knob residues (F350 and F351) with the idea being that if these knob residues are important for peptide activation than mutation of them should lead to a reduction of activity. Previous studies have indicated that this is indeed the case, as S1.6 displayed almost no activity—equivalent to that of the S1.3 derivative which lacks the knob residues entirely (Moon et al. 2015). Those results have lent credence to the theory that the phenylalanine knob residues of the synthetic peptides are important for the peptide mode of activation.

However, a later set of experiments showed that the Wolf4 peptide, a S1.5 derivative which possessed a double phenylalanine to alanine substitution within the knob residues, displayed activity equivalent to that of S1.5. This would appear to indicate that the phenylalanine residues are important for activation in the context of the full-length switch helix derivatives (S1.1, S1.6) but not important in the context of the truncated peptide derivatives (S1.5, Wolf4). These results were perplexing and required further exploration. In order to verify that S1.6 possessed no activity, activity was probed via the Normal radiometric kinase assay and displayed a  $K_a$  value of 11.4  $\mu\text{M}$  with a Hill slope of 1.3 (**Figure 3.2.2, Table 3.2.2**). These results present a stark dichotomy between the previous reports showing no activation and the current study displaying activation that rivals that of the purportedly most potent peptide, S1.5.

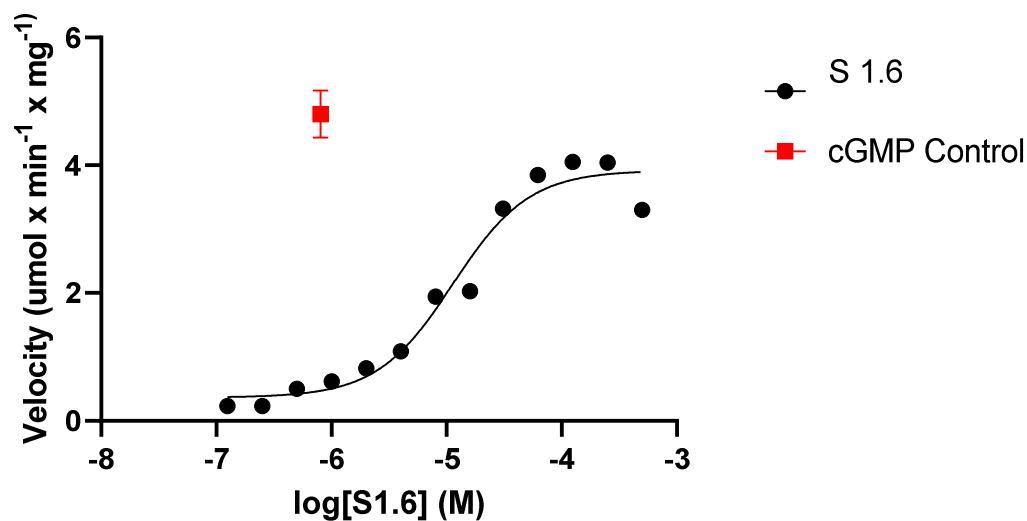


**Figure 3.2.2. S1.6-induced activation of PKG1- $\alpha$**

Activity of PKG1- $\alpha$  was measured at varying concentrations using the S1.6 peptide under the normal preincubation scheme (shown in black). X-axis concentrations are displayed as a logarithmic function of peptide concentration. A positive cGMP control (shown in red) was used at a concentration of 8  $\mu$ M, corresponding to known values of peak cGMP activation.

**Table 3.2.2. Activation kinetics of S1.6 under the normal preincubation scheme**

Name	$V_{\max}$	$V_{\min}$	$n_H$	$K_a$ [ $\mu$ M]	N
S1.6 Normal	$4.04 \pm 0.55$	$0.23 \pm 0.05$	1.31	$11.4 \pm 5.1$	4
cGMP	8.23	n/a	n/a	n/a	8

$n_H$ , Hill coefficient;  $K_a$ , activation constant; N, number of replicates. Velocity units are reported in  $\mu$ mol PKG-1 x min<sup>-1</sup> x mg<sup>-1</sup> substrate.

### 3.2.3 Wolf4

The Wolf4 peptide was probed in continuation of understanding the importance of the phenylalanine residues of the synthetic peptides. Differences in the activity of the S1.6 peptide reported in this thesis and past results required that the activity of the Wolf4 peptide be verified once again. The Wolf4 peptide was synthesized with the intention of probing the relevance of the phenylalanine residues within the context of the S1.5 peptide, parallel to the relation of the S1.1 and S1.6 peptides. The previously accepted hypothesis was that the phenylalanine's provided a hydrophobic interaction that was vital to the peptide pharmacophore. Ergo, substitution of these phenylalanine's should drastically reduce activity. However, that is not the case as Wolf4 appears to be the most potent peptide discovered thus far, possessing a  $K_a$  of 1.3  $\mu\text{M}$  and  $V_{\text{max}}$  of 7.97  $\mu\text{mol (w15-p)/min*mg}$  (**Figure 3.2.3, Table 3.2.3**).

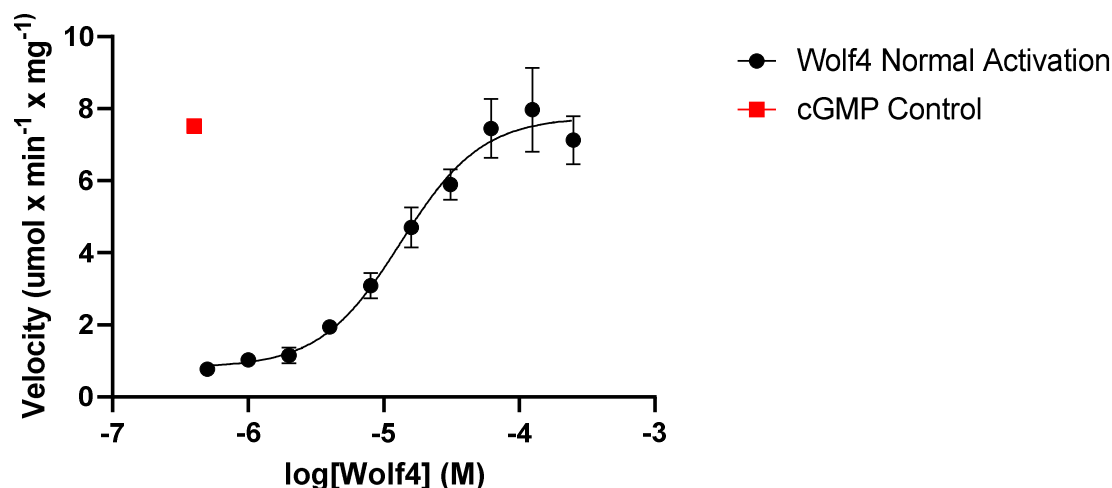


**Figure 3.2.3. Wolf4-induced activation of PKG1- $\alpha$**

Activity of PKG1- $\alpha$  was measured at varying concentrations using the Wolf4 peptide under the normal preincubation scheme (shown in black). X-axis concentrations are displayed as a logarithmic function of peptide concentration. A positive cGMP control (shown in red) was used at a concentration of 8  $\mu$ M, corresponding to known values of peak cGMP activation.

**Table 3.2.3. Activation kinetics of Wolf4 under the normal preincubation scheme**

Name	$V_{\max}$	$V_{\min}$	$n_H$	$K_a$ [ $\mu$ M]	N
Wolf4 Normal	$7.97 \pm 1.17$	$0.62 \pm 0.05$	1.46	$13.4 \pm 3.8$	4
cGMP	8.23	n/a	n/a	n/a	8

$n_H$ , Hill coefficient;  $K_a$ , activation constant; N, number of replicates. Velocity units are reported in  $\mu$ mol PKG-1 x min<sup>-1</sup> x mg<sup>-1</sup> substrate.

### **3.3.0 ATP Preincubation Method**

The revelation that the previously inactive S1.6 peptide now possesses activity posed a puzzling dilemma that warranted further investigation. It was discovered that there was a slight change in methodology between the assays being conducted in the initial experiments and those of present day. The radiometric kinase assays performed with the S1.5 and S1.5 derivative peptides had been done with a different preincubation scheme than that of the one that was used to probe activation kinetics of S1.6. With the S1.5 peptides, the enzyme was preincubated for 30 minutes at 30°C solely in the presence of EDB and the peptide stock and the reaction were initiated with a mixture of ATP, BSA, DTT, MES, ddH<sub>2</sub>O, and W15 substrate. However, the assays in the past with the S1.6 peptide were done by preincubating the enzyme in the presence of every single component, barring the ATP—which was used to start the reaction. A new set of experiments was designed in order to test whether this deviation in preincubation methodology was the causal factor for the difference in activity of the S1.6 peptide. These assays were conducted using the original preincubation scheme which had the enzyme preincubated in the presence of each reaction component aside from ATP.

### 3.3.1 S1.6

Activation of PKG by S1.6 is drastically reduced when switching to the ATP preincubation method. The activation constant becomes 31.3  $\mu\text{M}$ , a threefold increase from that of the normal preincubation scheme. In addition, the  $V_{\text{max}}$  drops to just 1.26  $\mu\text{mol (w15-p)/min}\cdot\text{mg}$  (Figure 3.3.1, Table 3.3.1). These results indicate a clear marked difference in activity between the two preincubation methods. Interestingly, the cGMP positive control remains at the same velocity irrespective of the preincubation method, indicating that the reduction in activity must be linked to the nature of the peptide itself.

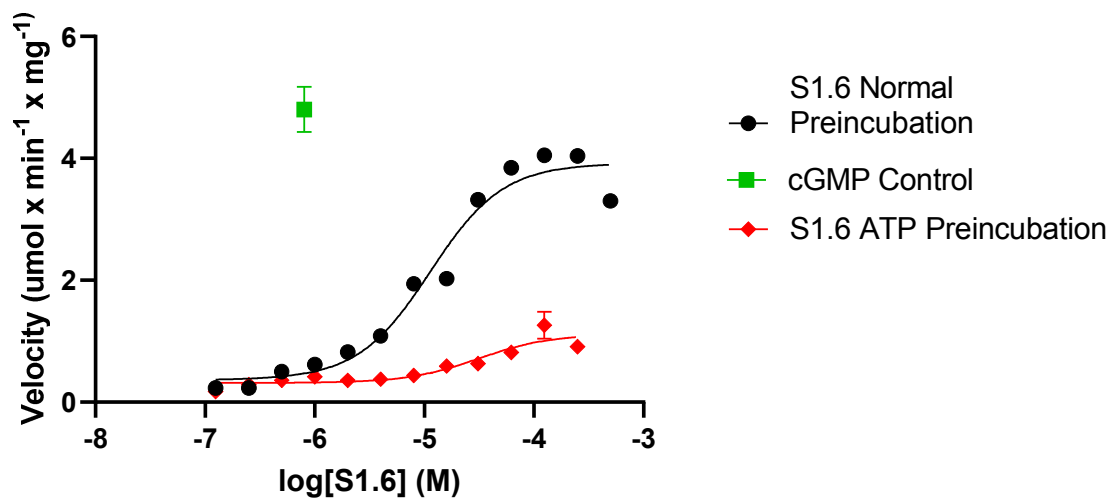


**Figure 3.3.1. A comparison of S1.6 activation curves under Normal and ATP activation**

Activity of PKG1- $\alpha$  was measured at varying concentrations using the S1.6 peptide under the normal preincubation scheme (shown in black) and the ATP preincubation scheme (shown in red). X-axis concentrations are displayed as a logarithmic function of peptide concentration. A positive cGMP control (shown in green) was used at a concentration of 8  $\mu\text{M}$ , corresponding to known values of peak cGMP activation.

**Table 3.3.1. Activation kinetics of S1.6 comparing the normal preincubation and ATP preincubation schemes**

<b>Name</b>	<b>V<sub>max</sub></b>	<b>V<sub>min</sub></b>	<b>n<sub>H</sub></b>	<b>K<sub>a</sub> [μM]</b>	<b>N</b>
S1.6 ATP	1.26 ± 0.22	0.18 ± 0.05	1.34	31.3 ± 7.3	4
S1.6 Normal	4.04 ± 0.55	0.23 ± 0.05	1.31	11.4 ± 5.1	4
cGMP	8.23 ± 0.37	n/a	n/a	n/a	8

n<sub>H</sub>, Hill coefficient; K<sub>a</sub>, activation constant; N, number of replicates. Velocity units are reported in μmol PKG-1 x min<sup>-1</sup> x mg<sup>-1</sup> substrate.

### 3.3.2 Wolf4

The Wolf4 peptide displays a similar decrease in activity when switching to the ATP preincubation method. There is a clear downward shift in PKG activity (**Figure 3.3.2**). The activation constant of Wolf4 is increased from 13.4 to 31.9  $\mu\text{M}$  and the  $V_{\text{max}}$  is decreased from 7.97 to 5.49  $\mu\text{mol (W15-p)}/\text{min}\cdot\text{mg}$  (**Table 3.3.2**).

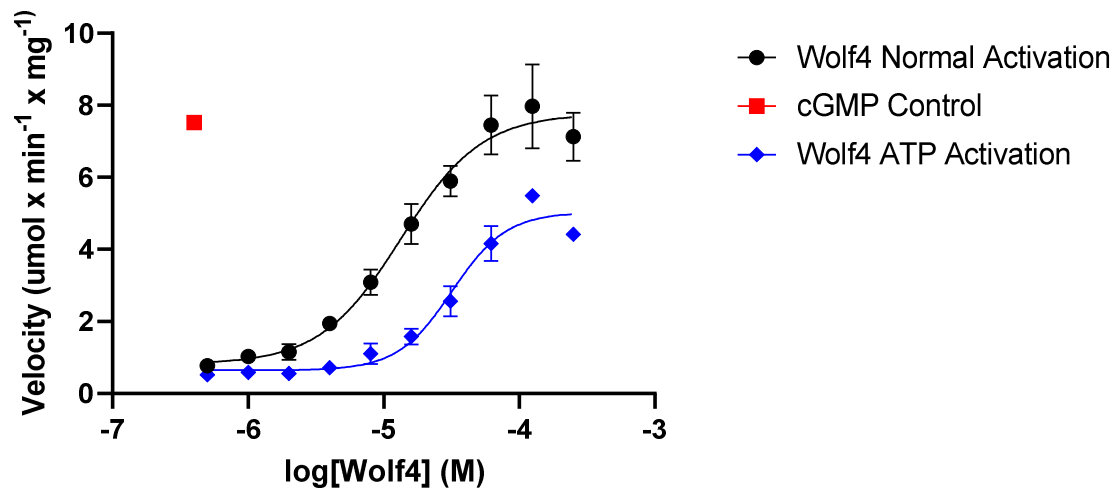


**Figure 3.3.2. A comparison of Wolf4 activation curves under Normal and ATP activation**

Activity of PKG1- $\alpha$  was measured at varying concentrations using the Wolf4 peptide under the normal preincubation scheme (shown in black) and the ATP preincubation scheme (shown in blue). X-axis concentrations are displayed as a logarithmic function of peptide concentration. A positive cGMP control (shown in red) was used at a concentration of 8  $\mu\text{M}$ , corresponding to known values of peak cGMP activation.

**Table 3.3.2. Activation kinetics of Wolf4 comparing the normal preincubation and ATP preincubation schemes**

<b>Name</b>	<b>V<sub>max</sub></b>	<b>V<sub>min</sub></b>	<b>n<sub>H</sub></b>	<b>K<sub>a</sub> [μM]</b>	<b>N</b>
Wolf4 ATP	5.49 ± 0.2	0.46 ± 0.08	2.167	31.9 ± 11.5	4
Wolf4 Normal	7.97 ± 1.17	0.62 ± 0.05	1.46	13.4 ± 4.1	4
cGMP	8.23 ± 0.11	n/a	n/a	n/a	8

n<sub>H</sub>, Hill coefficient; K<sub>a</sub>, activation constant; N, number of replicates. Velocity units are reported in μmol PKG-1 x min<sup>-1</sup> x mg<sup>-1</sup> substrate.

### 3.4 Dilution Assay

A possible explanation for the differing kinetic profiles between the different preincubation methods is that the concentrations of PKG1- $\alpha$  and S-tides are diluted in the less favorable ATP preincubation method in comparison to the Normal assay. It has been shown both by SPR and experimentally that S-tides possess a slow rate of association with PKG1- $\alpha$  with optimal preincubations needing between 15-30 mins at 30 °C (Moon et al. 2015, Charles 2019). It is possible that lowering the relative concentrations of PKG1- $\alpha$  and the respective S-tide would serve to further inhibit the peptide mode of association. Interestingly, the reduction in activity when utilizing the ATP preincubation method correlates nearly exactly with the ratio it is diluted by, with both being around 30%. A new preincubation scheme was developed to test this hypothesis. This dilution preincubation scheme was identical to the normal preincubation method with the only exception being that PKG and the synthetic peptide activator were preincubated at a threefold lower concentration. However, no significant differences were observed between the dilution assay and normal assay, ruling out the possibility that dilution of the preincubation mixture was the cause for the reduced activity shown in the ATP method of preincubation (**Figure 3.4, Table 3.4**).

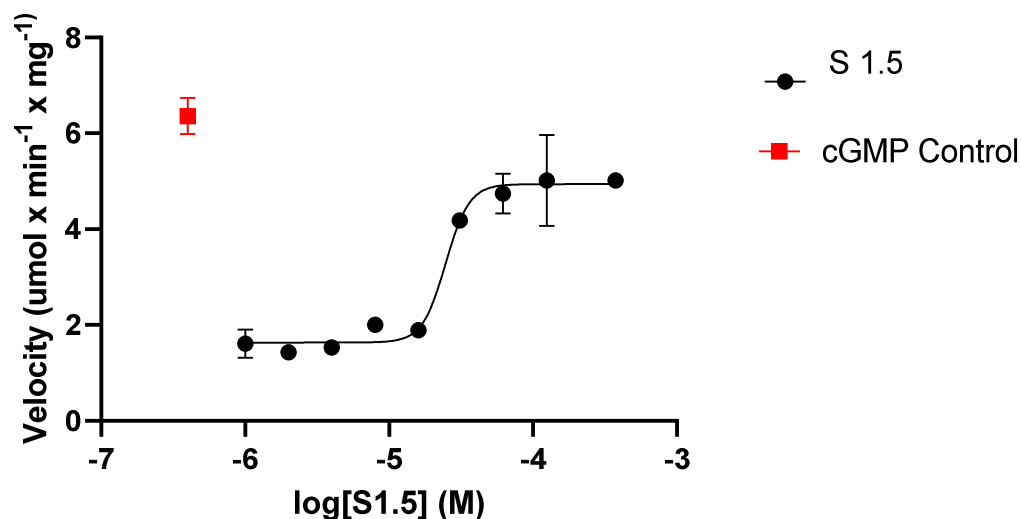


**Figure 3.4. S1.5-induced activation of PKG1- $\alpha$  under dilution conditions**

Activity of PKG1- $\alpha$  was measured at varying concentrations using the S1.5 peptide under the dilution preincubation scheme. X-axis concentrations are displayed as a logarithmic function of peptide concentration. A positive cGMP control (shown in red) was used at a concentration of 8  $\mu$ M, corresponding to known values of peak cGMP activation.

**Table 3.4. Activation kinetics of S1.5 comparing the dilution preincubation scheme and the normal preincubation.**

Name	$V_{max}$	$V_{min}$	$n_H$	$K_a$ [ $\mu$ M]	N
S1.5 Dilution	$5.02 \pm 0.14$	$1.43 \pm 0.17$	5.296	$24.8 \pm 4.4$	4
S1.5 Normal	$5.37 \pm 0.28$	$0.23 \pm 0.05$	4.18	$22.9 \pm 9.1$	6
cGMP	$6.34 \pm 0.38$	n/a	n/a	n/a	6

$n_H$ , Hill coefficient;  $K_a$ , activation constant; N, number of replicates. Velocity units are reported in  $\mu$ mol PKG-1 x  $min^{-1}$  x  $mg^{-1}$  substrate.

### **3.5. Isolating Assay Components**

Another possible explanation for the difference in kinetic activity between the two preincubation methods is that one or more components of the assay is behaving differently between the two methods. To test this hypothesis each component of the assay was moved piecewise from the activation mix to the preincubation mix (**Table 3.5**). Each permutation of the preincubation mix that did not contain MES showed a level of activity similar to the Normal preincubation method, whereas the preincubation mixes containing MES failed to activate PKG to any considerable level. These results indicate that the presence of the MES buffer within the preincubation mix drastically reduces S-tide-induced activity of PKG and is likely the component responsible for the shift in activity across the normal and ATP activation methods.

Preincubation Mixes							
PKG	S1.6 (61 $\mu$ M)	W15	BSA	DTT	ddH2O	MES	Status
x	x	x					Active
x	x	x	x				Active
x	x	x	x	x			Active
x	x	x	x	x	x		Active
x	x	x	x	x	x	x	Inactive
x	x	x		x	x	x	Inactive
x	x	x	x		x	x	Inactive
x	x		x	x	x	x	Inactive
x	x					x	Inactive
x	x	x	x	x	x		Active
x	x		x			x	Inactive
x	x		x	x			Inactive

**Table 3.5. Status of S1.6-induced PKG activation under varying preincubation conditions**

The relative activity of PKG is displayed after moving various components from the activation mix into the preincubation mix. Each row corresponds to a preincubation mix. The “x” mark in a column indicates the component is present in the preincubation mix. The green and red cells containing “Active” and “Inactive” indicate the relative level of PKG activation, with “Active” corresponding to a ten or higher fold of activation and “Inactive” corresponding to a two or lower fold of activation.

### **3.6 Deconstruction of the MES Buffer**

The MES buffer was deconstructed in a piecewise fashion identical to the preincubation isolation assays in (see **section 3.5.**) Results from this series of assays were graphed in normalized activation values and indicate two important findings (**Figure 3.6**). First, the magnesium is indeed crucial for the ATP catalysis and removal of magnesium from the assay completely negates activity. Secondly, there is a singular buffer component that is responsible for the drop in activity. The activity is reduced to 68.7% of the normal assay when the MgOAc is present in the preincubation mix and the other MES components are moved to the reaction mix. Furthermore, there is a similar decline in activity if there is no MES salt or NaCl in the assay at all and only the MgOAc is added into the preincubation mix. These results indicate that the MgOAc is the component of the buffer that is responsible for the decline in activity between the normal and ATP activation methods.

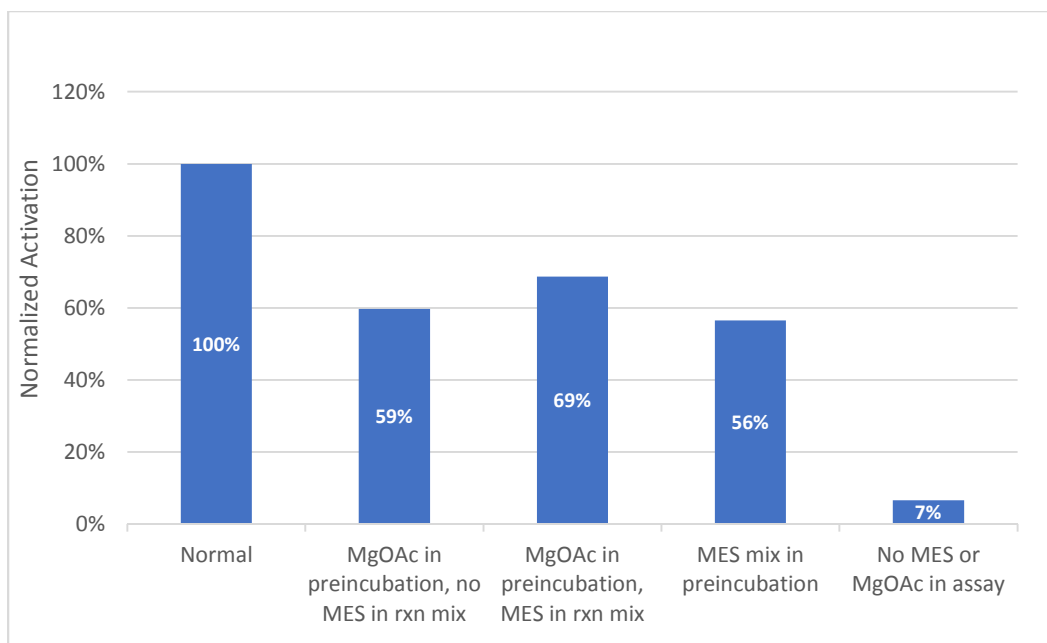


**Figure 3.6. Component Effects of MES Buffer**

Constitutive components of the MES buffer were shuffled around the preincubation and reaction mixes. The resulting activity was normalized and displayed in relative percentages. The X-axis labels indicate the composition of the assay with “MES mix” indicating all three components of the MES buffer (NaCl, MES salt, MgOAc). The “Normal” assay contains PKG and S1.6 in the preincubation mix and all other components in the reaction mix.

### 3.7 LSA-50 filter papers as an alternative to phosphocellulose

One of the principal benefits of using the radioactive kinase assay to measure PKG-1 activity is due to the relatively low cost of the required materials. However, recent radioactivity price hikes and an increasingly scarce demand of the required P81 filter papers have rendered the radioactive kinase assay less and less appealing and necessitated the exploration of alternative approaches. The discontinuation of P81 filter papers in particular justified an investigation into other suitable cation exchange papers and LSA-50 paper was deemed a suitable replacement. LSA-50 filter paper is similar to P81 papers in many regards and is significantly cheaper per mm<sup>2</sup>.

LSA-50 papers are strong cation exchangers and possess a polystyrene matrix that is crosslinked with divinylbenzene and contains sulfonate instead of phosphate groups as the active component (Appelmans et al. 2021). A full activity curve of S1.5-induced PKG-1 activation was done on both the LSA-50 and P81 filter papers in tandem to compare the two (**Figure 3.7**). Results from this experiment reveal a nearly identical activation profile between the two papers, suggesting that LSA-50 filter papers possess the chemical properties suitable for radioactive kinase assays. However, there are distinct physical differences between LSA-50 and P81 filter papers. The latter come in rectangular, easy to cut sheets whereas the LSA-50 papers come in circular pucks making it difficult to cut into efficient sections. Furthermore, the LSA-50 filters are far less durable than P81 papers and prone to tears. The reduced durability also inhibits the ability to effectively label the papers using a pen or pencil and even if accomplished the labels tend to drastically fade during the wash cycles of the assay. While it is technically possible to use LSA-50 as a replacement for P81, the frail nature of the paper poses significant problems and warrants use only out of necessitation.

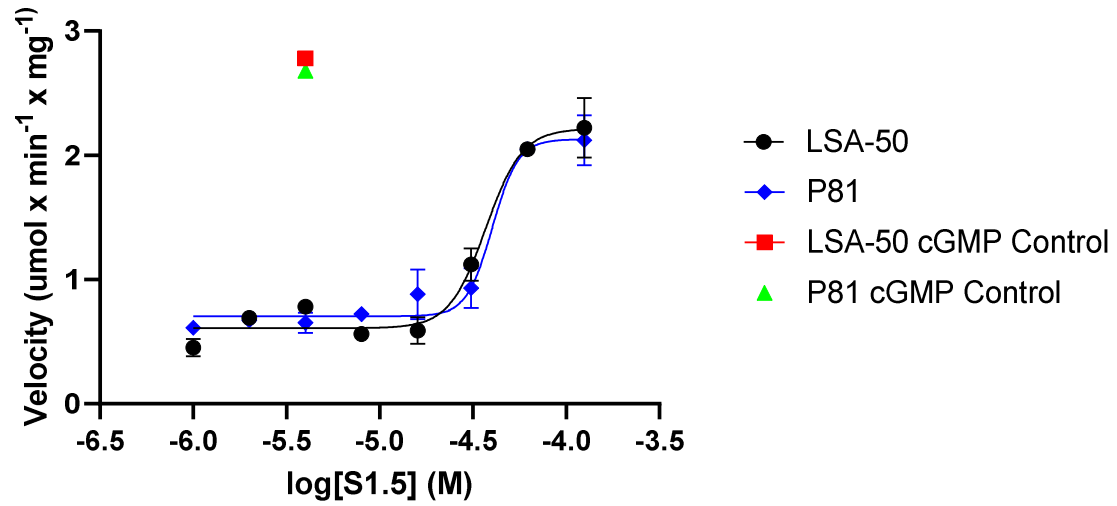


**Figure 3.7. Comparison of LSA-50 and P81 activation**

S.5-induced activity of PKG-1 is displayed as measured using the Normal preincubation scheme blotted onto LSA-50 (shown in black) and P81 phosphocellulose paper (shown in blue). X-axis concentrations are displayed as a logarithmic function of peptide concentration. A positive cGMP control (shown in red for LSA-50 and green for P81) was used at a concentration of 8  $\mu$ M, corresponding to known values of peak cGMP activation.

#### **4.0 Discussion**

The vasodilatory effects of the nitric oxide signaling pathway have long cemented it as a target of high interest for researchers developing therapeutics for the treatment of a broad spectrum of vascular pathophysiology's. However, of the various signaling molecules within the nitric oxide signaling pathway, there is yet to be a therapeutic specifically targeting PKG-1. To date, all nitric oxide signaling modulators on the market work by affecting intracellular levels of cGMP. This thesis seeks to expand upon the development of a new subclass of nitric oxide signaling modulators which explicitly target PKG-1, a novel approach to treating certain vascular pathologies such as hypertension.

The elucidation of the regulatory domain crystal structure of PKG-1 revealed a previously uncharacterized helical domain, dubbed the “switch helix,” that serves as a site of interprotomer communication. Mutational analysis of the switch helix knob residues within full-length PKG-1 revealed that disruption of this interprotomer interface leads to a decreased cGMP activation constant and allows PKG-1 to be more easily activated (Osborne et al. 2011). It was hypothesized that synthesis of the switch helix domain could perhaps serve the same purpose to disrupt this interprotomer interface and activate the kinase. Thus, the first synthetic peptide, S1.1, was synthesized. Remarkably, S1.1 was shown via surface plasmon resonance to associate with PKG-1 and then later on confirmed to elicit kinase activity (Moon et al. 2015). A series of synthetic peptide derivatives containing various truncations and substitutions were created to probe the nature of the S-tide pharmacophore and improve activity. The most potent of these derivatives was the S1.5 peptide, an N-terminally truncated version of the parent S1.1 compound (Moon et al. 2015).

#### 4.1 Assay Conditions Drastically Affect PKG-1 $\alpha$ activation

Although the synthetic peptides have been shown to be potent cGMP-independent activators of PKG-1, the nature of peptide-induced activation and the associated pharmacophore has yet to be elucidated. What little is known about the pharmacophore centers around two phenylalanine residues within the S-tides. These phenylalanine's reflect a portion of the hydrophobic knob residues within full-length PKG-1. Through the S1.6 peptide it was shown that substituting the phenylalanine residues abolishes S-tide activation, suggesting these residues must reflect a key portion of the pharmacophore (Moon et al. 2015). The initial goal of this thesis was to verify that hypothesis and validate whether it holds true within the context of the truncated S1.5 derivative. However, it was quickly discovered that the S1.6 peptide was not only active but displayed similar potency to that of S1.5, a peptide previously thought to be far more potent in comparison (**Table 3.2.1, Table 3.2.2**). This newfound activity poses a stark dichotomy to that of the activity previously published showing negligible S1.6-induced PKG-1 activation (Moon et al. 2015). Attempts to explain the inconsistency of S1.6 activity revealed a deviation of methodology in the previously published results displaying no activity. It was discovered that the previously published results had used a different preincubation scheme, one in which the preincubation mix contains all assay components and is initiated solely by [ $\gamma$ -<sup>32</sup>P]ATP. This preincubation scheme was replicated alongside the normal preincubation method and the results revealed a drastic difference in activity across the two schemes (**Figure 3.3.1**). This assay was replicated using a different peptide, Wolf4, revealing a similar shift in activity between the two preincubation methods (**Figure 3.3.2**).

## 4.2 Comparison of Preincubation Methods

Discovery of a difference in apparent activity across the ATP and normal preincubation methods was puzzling and warranted further investigation. Initially, it was hypothesized that the downward shift in activity displayed with the ATP preincubation method was a result of a dilution effect. In the normal assay, the preincubation mix consists of solely the kinase and the activator with a total volume of 30  $\mu\text{L}$ . Conversely, the ATP preincubation mix consists of the kinase, the activator, and all other assay components barring ATP for a total volume of 90  $\mu\text{L}$ . It is known that the synthetic peptides possess a relatively slow rate of association with PKG-1, as shown by surface plasmon resonance (Moon et al. 2015). Therefore, it's possible that the threefold higher preincubation volume impairs the ability for the synthetic peptides to associate with PKG-1. It was also observed that the activity is roughly threefold lower in the diluted ATP preincubation method, corresponding precisely with the dilution ratio. To test this hypothesis, a new assay was developed in which the preincubation method was similar to the normal method however all of the components were diluted threefold. Results from this assay were no different from the normal preincubation method, ruling out the possibility of a dilution effect being culpable for the shift in activity across assays (Figure 3.4.1).

### 4.3 Kinase Assay Deconstruction

Discovery that dilution of the preincubation mix had no effect on activity means that it can be reasonably assumed that the shift in activity across preincubation methods must be a result of either one or multiple components in the assay causing an unforeseen effect. Therefore, further attempts to explain the shift in activity was accomplished via a piecewise deconstruction of the assay. Each component of the assay was isolated and analyzed by moving components one at a time from the reaction mix to the preincubation mix. The activity of the kinase was observed for changes in each preincubation permutation and displayed in a matrix (**Figure 3.5**). Results from this assay deconstruction clearly point towards the MES buffer as being the component responsible for the shift in activity.

#### 4.4 Deconstruction of the MES Buffer

After identifying the MES buffer as being responsible for causing a drastic shift in activity, we were left positing how that could possibly be the case. The MES buffer is a morpholino salt derivative that was developed a so called “Good’s buffer” in the early 1960’s and is a staple in biological research (Good et al. 1966). The buffer used in the assays within this thesis contains 250mM of the MES salt (2-(N-morpholino) ethanesulfonic acid) as well as 50 mM NaCl and 5 mM MgOAc. The NaCl is added to reflect physiological salt levels whereas the purpose of the MgOAc is for the magnesium to act as a chelation agent to coordinate ATP during the phosphotransferase reaction (Buelens et al. 2021). The composite nature of the buffer meant that the activity shift could be a result of the MES salt itself, the NaCl, the MgOAc, or any combination of the aforementioned components. Therefore, a similar approach that was used to identify the MES buffer as the component responsible for the activity shift was used to identify which of the three buffer components was the contributing factor. Results from this approach indicate the MgOAc as the responsible component and show that the presence of MgOAc alone within the preincubation mix can reduce activity levels to that of 68.7% compared to the normal assay (**Figure 3.6**).

Logically, the drop in activity caused by the addition of MgOAc to the preincubation mix can be attributed to either a disruption of the enzyme, interference with the substrate, or interference with the activator. Because the cGMP control induces activity to the same degree across the two methods, we can rule out the possibilities of the enzyme or substrate being somehow impaired. Therefore, the difference in activity must be related to the S-tides. Although, precisely how MgOAc disrupts the S-tide induced activation is unknown and remains a topic for future investigation. One possible explanation is that the magnesium is binding to electronegative pockets provided by aspartate and glutamate that are 7 residues apart, coinciding with two turns of an  $\alpha$ -helix (**Figure 4.4**). Previous scanning-alanine mutagenesis results have shown that these electronegative residues are important for S-tide binding (Charles 2019). Therefore, if magnesium were to bind to the peptides in such fashion it would likely impair the S-tides ability to bind and activate PKG1- $\alpha$ ,

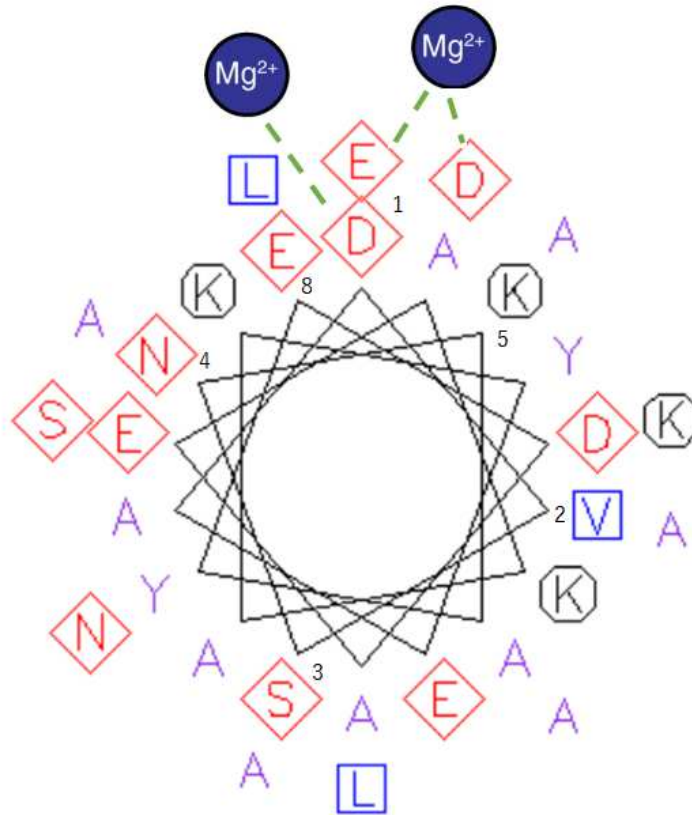


**Figure 4.4 Helix Wheel Depiction of S1.6**

The helix wheel diagram depicts the S1.6 peptide as if it were a barrel and one was looking at it from above, highlighting the spatial dynamics of side-chain amino acids that are 7 residues apart. Numbers correspond to C-termini residues of S1.6. Green dotted lines depict two pockets of electronegativity which allow for potential binding of magnesium.

#### **4.5 Revision of S-tide Pharmacophore**

Regardless of how the MgOAc disrupts the assay, the revelation that two similar yet distinct assay conditions can produce opposing results warrants a re-examination of all previous S-tide studies. All information available about the putative peptide pharmacophore must be scrutinized and compared within the context of the assay conditions that the data originates from. Previously, the two phenylalanine residues within the S-tides were thought to be a vital component of the pharmacophore. The work of this thesis posits a complete role-reversal of the importance of those residues. The revelation that the S1.6 peptide, which has both phenylalanine's substituted, possesses activity similar to S1.5 indicates that these two residues have gone from being a vital part of the supposed pharmacophore to being unimportant altogether. Although, it is important to consider that the method used to probe these residues was accomplished via alanine substitution. Like phenylalanine, alanine is a hydrophobic residue therefore it is possible that peptide activity remains equivalent because of the conserved hydrophobic nature of that portion of the peptide. Future experiments could explore that possibility by substituting the phenylalanine's with a non-hydrophobic residue or a charged residue such as aspartate or glutamine.

#### 4.6 Small Molecule Derivatives

An exciting future prospect for the targeted activation of PKG1- $\alpha$  lies within the development of small molecule agonists. Small molecules have many distinct advantages over peptide drugs, as peptide drugs typically have issues entering the target cells as well as provoking an immune response (Gokhale and Satyanarayanajois 2014). Recently, the Dostmann lab has partnered with the drug development company Cyclica to develop a series of small molecule agonists of PKG1- $\alpha$  via an *in silico* approach. Cyclica's proprietary MatchMaker™ software screened a 2.7 million compound library against PKG1- $\alpha$ , resulting in the identification of 279 optimal compounds that have high likelihood of binding to PKG1- $\alpha$ . These compounds have been predicted to bind with varying affinities to three distinct pockets located within the vicinity of the nest region. Activity of these compounds will be screened via the radioactive kinase assay. If one of these compounds is identified as a potent activator of PKG1- $\alpha$  then it could potentially have clinical significance as an anti-hypertensive.

## 5.0 REFERENCES

- Appelmans, O., R.S. Kashyap, P. Gilles, W.M. De Borggraeve, and J. Van Lint A. Voet. 2021. "LSA-50 paper: An alternative to P81 phosphocellulose paper for radiometric protein kinase assays." *Analytical Biochemistry*. doi: <https://doi.org/10.1016/j.ab.2021.114313>.
- Buelens, Floris P., Hadas Leonov, Bert L. de Groot, and Helmut Grubmüller. 2021. "ATP–Magnesium Coordination: Protein Structure-Based Force Field Evaluation and Corrections." *Journal of Chemical Theory and Computation* 17 (3):1922-1930. doi: 10.1021/acs.jctc.0c01205.
- Butt, E., J. Geiger, T. Jarchau, S. M. Lohmann, and U. Walter. 1993. "The cGMP-dependent protein kinase--gene, protein, and function." *Neurochem Res* 18 (1):27-42. doi: 10.1007/bf00966920.
- Charles, Joseph William author. 2019. *Studies on the Molecular Mechanism of S-Tide Mediated Activation of PKG-I[alpha] / Joseph William Charles*. Edited by Pharmacology University of Vermont. Department of.
- Das, Anindita, Arun Samidurai, Nicholas N. Hoke, Rakesh C. Kukreja, and Fadi N. Salloum. 2015. "Hydrogen sulfide mediates the cardioprotective effects of gene therapy with PKG- $\alpha$ ." *Basic Research in Cardiology* 110 (4):42. doi: 10.1007/s00395-015-0500-y.
- Dostmann, Wolfgang R. G., Christian Nickl, Stefan Thiel, Igor Tsigelny, Ronald Frank, and Werner J. Tegge. 1999. "Delineation of Selective Cyclic GMP-Dependent Protein Kinase  $\alpha$  Substrate and Inhibitor Peptides Based on Combinatorial Peptide Libraries on Paper." *Pharmacology & Therapeutics* 82 (2):373-387. doi: [https://doi.org/10.1016/S0163-7258\(98\)00063-1](https://doi.org/10.1016/S0163-7258(98)00063-1).
- Francis, Sharron H., Jennifer L. Busch, Jackie D. Corbin, and David Sibley. 2010. "cGMP-dependent protein kinases and cGMP phosphodiesterases in nitric oxide and cGMP action." *Pharmacological reviews* 62 (3):525-563. doi: 10.1124/pr.110.002907.
- Glass, D. B., R. A. Masaracchia, J. R. Feramisco, and B. E. Kemp. 1978. "Isolation of phosphorylated peptides and proteins on ion exchange papers." *Anal Biochem* 87 (2):566-575. doi: 10.1016/0003-2697(78)90707-8.
- Gokhale, Ameya S., and Seetharama Satyanarayanajois. 2014. "Peptides and peptidomimetics as immunomodulators." *Immunotherapy* 6 (6):755-774. doi: 10.2217/imt.14.37.
- Good, Norman E., G. Douglas Winget, Wilhelmina Winter, Thomas N. Connolly, Seikichi Izawa, and Raizada M. M. Singh. 1966. "Hydrogen Ion Buffers for Biological Research\*." *Biochemistry* 5 (2):467-477. doi: 10.1021/bi00866a011.
- Gremer, Sebastian. 2019. "Oxidation of PKG  $\alpha$  C42 Potentiates Kinase Activation by Cyclic Nucleotides." *Free radical biology & medicine* 145:S112-S113. doi: 10.1016/j.freeradbiomed.2019.10.301.
- Horowitz, Arie, Constance B. Menice, Regent Laporte, and Kathleen G. Morgan. 1996. "Mechanisms of smooth muscle contraction." *Physiological Reviews*, 1996/10//, 967+.
- Kyle, Barry D., Soleil Hurst, Richard D. Swayze, Jianzhong Sheng, and Andrew P. Braun. 2013. "Specific phosphorylation sites underlie the stimulation of a large conductance, Ca<sup>2+</sup>-activated K<sup>+</sup> channel by cGMP-dependent protein kinase." *The FASEB journal* 27 (5):2027-2038. doi: 10.1096/fj.12-223669.
- Larsen, Torben. 2005. "Determination of lactate dehydrogenase (LDH) activity in milk by a fluorometric assay." *Journal of Dairy Research* 72 (2):209-216. doi: 10.1017/S0022029905000865.
- Lee, Meng-Luen, Erna Sulistyowati, Jong-Hau Hsu, Bo-Yau Huang, Zen-Kong Dai, Bin-Nan Wu, Yu-Ying Chao, and Jwu-Lai Yeh. 2019. "KMUP-1 Ameliorates Ischemia-Induced

- Cardiomyocyte Apoptosis through the NO<sup>-</sup>cGMP<sup>-</sup>MAPK Signaling Pathways." *Molecules* 24 (7):1376. doi: 10.3390/molecules24071376.
- Light, Douglas B., Bruce A. Stanton, and Jackie D. Corbin. 1990. "Dual ion-channel regulation by cyclic GMP and cyclic GMP-dependent protein kinase." *Nature* 344 (6264):336-339. doi: 10.1038/344336a0.
- Moon, Thomas M., Jessica L. Sheehe, Praveena Nukareddy, Lydia W. Nausch, Jessica Wohlfahrt, Dwight E. Matthews, Donald K. Blumenthal, and Wolfgang R. Dostmann. 2018. "An N-terminally truncated form of cyclic GMP-dependent protein kinase I $\alpha$  (PKG I $\alpha$ ) is monomeric and autoinhibited and provides a model for activation." *J Biol Chem* 293 (21):7916-7929. doi: 10.1074/jbc.RA117.000647.
- Moon, Thomas M, Nathan R Tykocki, Jessica L Sheehe, Brent W Osborne, Werner Tegge, Joseph E Brayden, and Wolfgang R Dostmann. 2015. "Synthetic Peptides as cGMP-Independent Activators of cGMP-Dependent Protein Kinase I $\alpha$ ." *Chem Biol* 22 (12):1653-1661. doi: 10.1016/j.chembiol.2015.11.005.
- Nalli, Ancy D., Divya P. Kumar, Othman Al-Shboul, Sunila Mahavadi, John F. Kuemmerle, John R. Grider, and Karnam S. Murthy. 2014. "Regulation of G $\beta$ yi-Dependent PLC- $\beta$ 3 Activity in Smooth Muscle: Inhibitory Phosphorylation of PLC- $\beta$ 3 by PKA and PKG and Stimulatory Phosphorylation of Gai-GTPase-Activating Protein RGS2 by PKG." *Cell Biochemistry and Biophysics* 70 (2):867-880. doi: 10.1007/s12013-014-9992-6.
- Nausch, Lydia Waltraud Maria. 2008. "Novel insights to PKG activation and cGMP signaling in response to nitric oxide and atrial natriuretic peptide in vascular smooth muscle cells / by Lydia Waltraud Maria Nausch." Thesis (PhD)--University of Vermont, 2008.
- Osborne, Brent W, Jian Wu, Caitlin J McFarland, Christian K Nickl, Banumathi Sankaran, Darren E Casteel, Virgil L Woods, Alexandr P Kornev, Susan S Taylor, and Wolfgang R Dostmann. 2011. "Crystal Structure of cGMP-Dependent Protein Kinase Reveals Novel Site of Interchain Communication." *Structure* 19 (9):1317-1327. doi: 10.1016/j.str.2011.06.012.
- Plüger, Saskia, Jörg Faulhaber, Michael Fürstenau, Matthias Löhn, Ralph Waldschütz, Maik Gollasch, Hermann Haller, Friedrich C. Luft, Heimo Ehmke, and Olaf Pongs. 2000. "Mice With Disrupted BK Channel  $\beta$ 1 Subunit Gene Feature Abnormal Ca<sup>2+</sup> Spark/STOC Coupling and Elevated Blood Pressure." *Circulation* 102 (11):e53-e60. doi: 10.1161/01.RES.87.11.e53.
- Rigatti, Marc, Andrew V. Le, Claire Gerber, Ion I. Moraru, and Kimberly L. Dodge-Kafka. 2015. "Phosphorylation state-dependent interaction between AKAP7 $\delta$ / $\gamma$  and phospholamban increases phospholamban phosphorylation." *Cellular Signalling* 27 (9):1807-1815. doi: <https://doi.org/10.1016/j.cellsig.2015.05.016>.
- Salb, Katharina, Elisabeth Schinner, and Jens Schlossmann. 2011. "Function of IRAG and the phosphorylation of the InsP3R-I for the NO/cGMP-dependent inhibition of platelet aggregation." *BMC pharmacology* 11 (S1):P58-P58. doi: 10.1186/1471-2210-11-S1-P58.
- Sasaki, T., K. Kawai, K. Saijo-Kurita, and T. Ohno. 1992. "Detergent cytotoxicity: simplified assay of cytolysis by measuring LDH activity." *Toxicology in Vitro* 6 (5):451-457. doi: [https://doi.org/10.1016/0887-2333\(92\)90052-S](https://doi.org/10.1016/0887-2333(92)90052-S).
- Schnell, Jason R., Guo-Ping Zhou, Markus Zweckstetter, Alan C. Rigby, and James J. Chou. 2005. "Rapid and accurate structure determination of coiled-coil domains using NMR dipolar couplings: Application to cGMP-dependent protein kinase I $\alpha$ ." *Protein science* 14 (9):2421-2428. doi: 10.1110/ps.051528905.
- Sellak, Hassan, Chung-sik Choi, Nupur B. Dey, and Thomas M. Lincoln. 2012. "Transcriptional and post-transcriptional regulation of cGMP-dependent protein kinase (PKG-I):

pathophysiological significance." *Cardiovascular Research* 97 (2):200-207. doi: 10.1093/cvr/cvs327.

Tamura, Naohisa, Hiroshi Itoh, Yoshihiro Ogawa, Osamu Nakagawa, Masaki Harada, Tae-Hwa Chun, Shin-ichi Suga, Takaaki Yoshimasa, and Kazuwa Nakao. 1996. "cDNA Cloning and Gene Expression of Human Type I alpha cGMP-Dependent Protein Kinase." *Hypertension (Dallas, Tex. 1979)* 27 (3):552-557. doi: 10.1161/01.HYP.27.3.552.

Wolfe, L., S. H. Francis, and J. D. Corbin. 1989. "Properties of a cGMP-dependent monomeric protein kinase from bovine aorta." *J Biol Chem* 264 (7):4157-4162. doi: 10.1016/S0021-9258(19)84976-1.

Zhao, Yidan D., Lei Cai, Muhammad K. Mirza, Xiaojia Huang, Dave L. Geenen, Franz Hofmann, Jason X. J. Yuan, and You-Yang Zhao. 2012. "Protein Kinase G-I Deficiency Induces Pulmonary Hypertension through Rho A/Rho Kinase Activation." *Am J Pathol* 180 (6):2268-2275. doi: 10.1016/j.ajpath.2012.02.016.